

2023

## The influence of using HHO with sunflower and soybean oil biodiesel/diesel blend on PCCI engine characteristics

Mai H. Aboubakr

*Faculty of Engineering, Tanta University, mai160584@f-eng.tanta.edu.eg*

Medhat Elkelawy Prof. Dr.

*Faculty of Engineering, Tanta University, medhatelkelawy@f-eng.tanta.edu.eg*

Hagar Alm-Eldin Bastawissi Prof. Dr.

*Faculty of Engineering, Tanta University, hagaralmeldin@f-eng.tanta.edu.eg*

Ayman R. El-Tohamy Dr.

*Faculty of Engineering, Tanta University, Ayman.Refaat@f-eng.tanta.edu.eg*

Follow this and additional works at: <https://digitalcommons.aaru.edu.jo/erjeng>



Part of the [Mechanical Engineering Commons](#)

---

### Recommended Citation

Aboubakr, Mai H.; Elkelawy, Medhat Prof. Dr.; Bastawissi, Hagar Alm-Eldin Prof. Dr.; and El-Tohamy, Ayman R. Dr. (2023) "The influence of using HHO with sunflower and soybean oil biodiesel/diesel blend on PCCI engine characteristics," *Journal of Engineering Research*: Vol. 7: Iss. 6, Article 6.

Available at: <https://digitalcommons.aaru.edu.jo/erjeng/vol7/iss6/6>

This Article is brought to you for free and open access by Arab Journals Platform. It has been accepted for inclusion in Journal of Engineering Research by an authorized editor. The journal is hosted on [Digital Commons](#), an Elsevier platform. For more information, please contact [rakan@aarj.edu.jo](mailto:rakan@aarj.edu.jo), [marah@aarj.edu.jo](mailto:marah@aarj.edu.jo), [u.murad@aarj.edu.jo](mailto:u.murad@aarj.edu.jo).

# The influence of using HHO with sunflower and soybean oil biodiesel/diesel blend on PCCI engine characteristics

Mai H. Aboubakr<sup>\*1</sup>, Medhat Elkelawy<sup>2</sup>, Hagar Alm-Eldin Bastawissi<sup>3</sup>, Ayman R. El-Tohamy<sup>4</sup>

<sup>1</sup> Mechanical Power Engineering Departments, Faculty of Engineering, Tanta University, Tanta, Egypt – email: [Mai160584@f-eng.tanta.edu.eg](mailto:Mai160584@f-eng.tanta.edu.eg)

<sup>2</sup> Mechanical Power Engineering Departments, Faculty of Engineering, Tanta University, Tanta, Egypt – email: [medhatelkelawy@f-eng.tanta.edu.eg](mailto:medhatelkelawy@f-eng.tanta.edu.eg)

<sup>3</sup> Mechanical Power Engineering Departments, Faculty of Engineering, Tanta University, Tanta, Egypt – email: [hagaralmeldin@f-eng.tanta.edu.eg](mailto:hagaralmeldin@f-eng.tanta.edu.eg)

<sup>4</sup> Mechanical Power Engineering Departments, Faculty of Engineering, Tanta University, Tanta, Egypt – email: [Ayman.Refaat@f-eng.tanta.edu.eg](mailto:Ayman.Refaat@f-eng.tanta.edu.eg)

**Abstract-** This research studies the influence of various blends of sunflower and soybean oil biodiesel with diesel fuel on premixed charge compression engine characteristics, including performance and exhaust emissions, and also investigates the impact caused by oxyhydrogen gas addition on them. The experiments were carried out on a single cylinder PCCI engine which utilizing eight blends of the fuels. Conventional diesel, B20D80, B40D60, B60D40, B80D20, B40D60 + 5 LPM HHO, B40D60 + 10 LPM HHO, and B40D60 + 15 LPM HHO have been used to obtain performance and exhaust emissions characteristics. The hydrogen peroxide additive has introduced into the engine manifold while the diesel/biodiesel fuel blends have been injected directly into the engine cylinder. The results of the studies showed that adding a 40% biodiesel and 60% diesel blend to oxyhydrogen with flow rates of 15 LPM improved the performance characteristics as well as lower exhaust emissions characteristics when compared to the other seven blends. In contrast, conventional diesel had much higher exhaust emissions parameters.

**Keywords:** Oxyhydrogen [HHO], Biodiesel/diesel blends, Biodiesel production, PCCI Engine, Performance characteristics, Exhaust emissions characteristics, CI engine.

## Abbreviations/Nomenclature

CI	Compression engine
PCCI	Premixed charge compression engine
HHO	Oxyhydrogen gas
D100	Conventional diesel fuel
B20D80	20% biodiesel and 80% diesel blend
B40D60	40% biodiesel and 60% diesel blend
B60D40	60% biodiesel and 40% diesel blend
B80D20	80% biodiesel and 20% diesel blend
B40D60 + 5 LPM HHO	40% biodiesel, 60% diesel, and oxyhydrogen with 5 LPM
B40D60 + 10 LPM HHO	40% biodiesel, 60% diesel, and oxyhydrogen with 10 LPM
B40D60 + 15 LPM HHO	40% biodiesel, 60% diesel, and oxyhydrogen with 15 LPM

LPM	Liter per minute
TDC	Top dead center
°CA	Degree crank angle
g/kw.hr	Gram per kilowatt hour
°C	Degree Celsius
PPM	Parts per million
BTE	Brake thermal efficiency
BSFC	Brake specific fuel consumption
EGT	Exhaust gas temperature
HC	Hydrocarbon
CO <sub>2</sub>	Carbon dioxide
CO	Carbon monoxide
O <sub>2</sub>	Oxygen rate
NO <sub>x</sub>	Nitrogen oxide
NO	Nitric Oxide
NO <sub>2</sub>	Nitrogen Dioxide
SOOT	Smoke intensity
NaOH	Sodium Hydroxide
KOH	Potassium Hydroxide

## I. INTRODUCTION

In modern times, the world tends to prefer using renewable energy resources instead of fossil fuels [non-renewable energy resources] due to their negative impacts on humans and the environment [1-4]. Further, the main challenges that prompted the researchers to search for renewable energy sources to utilize as an alternative for fossil fuels [non-renewable sources] were the greenhouse effect and global warming [5].

Hydrogen fuel is one example of an alternative to fossil fuel because it is a renewable and sustainable energy source [6, 7]. Also, it is free carbon that led to a decrease in carbon dioxide emissions, non-toxic emissions, and assisted in reducing the increase of the world temperature to 2 °C, so hydrogen is called green hydrogen [8]. However, the challenge of hydrogen gas storage limits the use of pure hydrogen in diesel engines; therefore, the challenges of storing hydrogen have been solved to a certain extent by utilizing an oxyhydrogen [HHO], which is produced by applying a water electrolysis process with an electrolyte type [NaOH or KOH]. In addition, HHO contains two hydrogen and one oxygen, so it is like hydrogen: free carbon, an eco-friendly, sustainable source [9, 10]. Moreover, the main problem that was faced when adding HHO to biodiesel, diesel, or gasoline fuels was an increase in NOx emission levels, so researchers tend to solve this problem by using PCCI or HCCI engines [11]. The PCCI combustion technique combines the advantages of both spark-ignition [SI] and compression ignition direct injection [CIDI] engines [12-14]. The PCCI engine's combustion rule operates in lean fuel conditions. The dynamics of the reaction and its response rates to the behaviors of the mixed mixture control the burning and combustion processes [15-17]. As a result, managing the auto-ignition time and combustible mixture consumption rate in the PCCI engine is more difficult than in a conventional diesel engine [2].

Previous research studies on the addition of biodiesel and diesel mixes with HHO gas, as well as the usage of a PCCI engine on them, are discussed below [18-20]. The effect of mixing HHO with a 20% Bauhinia variegata biodiesel/diesel mix on combustion, performance, and emission parameters in a CI engine was investigated [21]. According to the findings, B20 reduces PCP and HRR by 15% and 24%, respectively. The biggest PCP increased by 11.5–13.5% compared to B20 with HHO flow rates of 3 LPM and 4 LPM, while the maximum HRR was found at B20 with HHO flow rates of 6 LPM [22]. When compared to diesel fuel, B20 lowered BTE by 7% and boosted BSFC by 11%. While the HHO flow rate of 3LPM was mixed with B20, the BTE increased by about 14%, but the BSFC decreased by about 7%, whereas for both BTE and BSFC, 4 LPM was closed to 3 LPM. CO and HC levels were lowered by 17% and 12%, respectively, at B20 as compared to diesel fuel. In the HHO and B20 mix, CO and HC both decreased, with the largest average CO reduction of 29% for a 3 LPM flow rate of HHO as near as 4 LPM; however, CO rose, as HHO was 6 LPM. The highest average HC decrease is about 24% for B20 with HHO flow rates of 3 LPM and 4 LPM. In all test conditions, NOx was incremental, and NOx levels went up 7% for B20. The flow rate of HHO increased by around 7–17% from 1 LPM to 6 LPM.

The impact of adding HHO to both 20% and 40% M. oleifera biodiesel and diesel mixtures on performance, combustion, and emission parameters for CI engine was studied [23]. The BTE at the HHO and B20 blend was higher than the D100 until 80% engine load; nevertheless, there was a 1% reduction at the maximum load when engine load rose. BSFC declined drastically as engine loads rose [24, 25]. When comparing the HHO and B20 blend to other test mixes, both cylinder pressure and EGT rose. As engine load rose, the HHO with B20 and B40 blends lowered the values of CO, CO<sub>2</sub>, and HC emissions, whereas NO<sub>x</sub> increased as engine load rose, although the HHO and B20 blend declined more than D100 at lower engine loads [26, 27].

The performance, emission, and combustion parameters of 25% and 50% of orange oil methyl ester biodiesel and diesel mix with and without hydroxyl [O25, O50, O25 +HHO, and O50 +HHO] on diesel engine were evaluated [28]. BTE declined by 6.9% and 10.06% at O25 and O50 but climbed by 9.08% and 3.54% at O25 + HHO and O50 + HHO, while BSFC increased by 3.7% and 7.4% at O25 and O50, respectively [29]. The lowest BSFC value at O25 + HHO is 14.28%, which is considerably less than both O25 and O50. Furthermore, cylinder pressure and HRR rose, and ignition delay was reduced at both blends of HHO plus O25 and HHO plus O50; however, cylinder pressure and HRR decreased, and ignition delay increased at O25 and O50. PCP values were 69.04, 65.89, 64.67, 70.81, and 68.07 bar at diesel, O25, O50, O25 + HHO, and O50 + HHO, respectively [30, 31]. The highest cylinder pressure and heat release values were achieved at 70.81 bar and 82.05 kJ/m<sup>3</sup>-deg. for O25 + HHO, respectively, whilst the lowest results were obtained at 64.7 bar and 68.14 kJ/m<sup>3</sup>-deg. at O50, respectively. CO, HC, and smoke emission decreased for O25, O50, O25 + HHO, and O50 + HHO, with the exception of NO<sub>x</sub>, which rises when O25 + HHO. O25 had a lower CO than O50, which lowered CO by 16.6% at O25 as compared to diesel at full load. Therefore, both O25 and O50 indicate a significant decrease in HC and smoke emission with 7.8 and 7.1%, and 2.6 and 4.8%, and an increase in NO<sub>x</sub> with 4.16 and 1.64%, respectively [32, 33]. The CO and smoke emission values of O25 + HHO and O50 + HHO are lowered by 15.46 and 5.76% and 18.2 and 4.21%, respectively, as compared with O25 and O50. Also, HC is less than diesel at O25 + HHO by 17.6% and O50 + HHO by 13.1% at 100% engine load. NO<sub>x</sub> had a considerable increase of 9.67% of O25 + HHO more than diesel fuel, which can be reduced via the EGR method.

The effect of using 30% waste cooking oil biodiesel and 70% diesel blend in the two running modes [CDC mode and various premixed concentrations of 15, 20, 25, and 30% diesel vapor with PCCI mode] was shown [34]. In the CDC mode, BSFC, NO<sub>x</sub>, and smoke opacity improved while BTE, EGT, HC, and CO declined. In PCCI mode, for performance parameters, the BTE raised but dropped both BSFC and EGT as premixed concentrations were 15, 20, and

25%, whilst 30% of premixed concentration observed a lower BTE and EGT but enhanced BSFC [35, 36]. In terms of emissions parameters, CO, HC, smoke opacity, and NO<sub>x</sub> decreased at premixed concentrations of 15, and 20%, while increasing CO, HC, and smoke opacity but dropping NO<sub>x</sub> at premixed concentrations of 25, and 30% for emissions parameters [37, 38].

The experiment results of additional bioethanol fuel with three percentages of 10%, 20%, and 30% injected in PCCI mode into wheat germ oil driven in a CI engine to output the engine parameters as performance, combustion, and exhaust emissions at different loads were demonstrated [39]. When the engine loads grew, then the performance parameters [BTE and EGT] were incremental, with 28.78% and 471 °C of diesel, 26.79% and 521 °C of wheat germ oil, 26.99% and 508 °C of bio-ethanol with varied percentages 10% plus wheat germ oil, 27.52% and 487 °C of bio-ethanol with varied percentages 20% plus wheat germ oil, and 28.14% and 471 °C of bio-ethanol with varied percentages 30% plus wheat germ oil, respectively, at full load [40, 41]. Further, increasing the percentage of bioethanol in wheat germ oil led to an increase in BTE and a decrease in EGT. When the engine was running incrementally, the peak in-cylinder pressure and combustion duration both increased, but the ignition delay decreased, and the heat release rate had an unstable curve. The peak in-cylinder pressure of diesel fuel was 70.5 bar greater than that of wheat germ oil, wheat germ oil + 10% bioethanol, wheat germ oil + 20% bioethanol, and wheat germ oil + 30% bioethanol, which were 62.4, 64.7, 65.9, and 67.6 bar, respectively. The highest and lowest heat release rate records were discovered at diesel and wheat germ oil, respectively, meanwhile heat release rate values had a remarkable increase when the amount of bioethanol that is added to wheat germ oil rose, which results even got very near to diesel performance.

Wheat germ oil had a higher ignition delay and combustion duration of 13 °CA and 59 °CA, respectively, than diesel, which is recorded at 10 °CA for ignition delay and 53 °CA for combustion duration, with the addition of an increase in the percentages of bioethanol that is added to wheat germ oil that caused a significant decline in both ignition delay and combustion duration. At the maximum point of the engine load, there was a remarkable reduction in combustion duration as the percentages of bioethanol plus wheat germ oil rose, with values of 57°CA for wheat germ oil + 10% bioethanol, 55°CA for wheat germ oil + 20% bioethanol, and 52°CA for wheat germ oil + 30% bioethanol[42, 43]. The curves of HC and smoke emissions grew as engine loads rose. On the other hand, the NO curve was considerably high until about 5 KW of engine load was reached, after which it dropped. As well as that, the CO curve increased almost to 2.7 KW before decreasing approximately to 3.3 KW following the upward trend [44, 45]. The obtained results of exhaust emissions [HC, CO, and

NO] found 171 ppm, 0.42%, and 923 ppm of diesel, 257 ppm, 0.74%, and 813 ppm of wheat germ oil, 235 ppm, 16%, and 782 ppm of wheat germ oil + 10% bioethanol, 231 ppm, 23%, and 774 ppm of wheat germ oil + 20% bioethanol, and 193 ppm, 35%, and 756 ppm of wheat germ oil + 30% bioethanol, respectively. Additionally, the addition of bioethanol fuel to wheat germ oil reduced HC, NO, and smoke due to the beneficial properties of bioethanol fuel [46-49]. The effect of varying premixed proportions [10%, 20%, and 30%] when added to a 30% waste cooked oil biodiesel and diesel blend utilizing a PCCI engine was explained [50]. This resulted in an enhancement in the BTE value and, on the contrary, a diminishment in the BSEC, CO, NO<sub>x</sub>, UHC, and smoke opacity values[51-53].

The influences of adding 30% premixed proportions to two different mixtures of waste cooked oil biodiesel and diesel [B40] on the PCCI-Diesel engine as compared to the observed results with the diesel engine were explored [10]. The average BTE value achieved by applying it to the PCCI-Diesel engine with B40 at 30% premixed proportion raised from 19.34% to 29.91% when compared to the diesel engine [54-56]. On the contrary, the addition of 30% premixed proportion to 40% of waste cooked oil biodiesel and diesel mixes caused a reduction in BSEC and EGT of 22.22% and 29.36%, respectively, as compared to the diesel engine. Moreover, both peak in-cylinder pressure and heat release rate increased noticeably after adding 30% premixed proportion to 40% waste cooking oil biodiesel and diesel mixtures, but the PCCI-DI engine had a considerable drop in exhaust emissions [UHC, CO, NO<sub>x</sub>, and smoke opacity] of 42.42%, 66.93%, 61.89%, and 66%, respectively, for blends of 30% premixed proportion and 40% waste cooking oil biodiesel/diesel mixtures when compared to the diesel engine [57, 58].

The authors carried out experiments to discover the most optimal blend and catalyst test to gain improved performance and less emissions by differing the amounts of microalgae biodiesel and diesel with CuO nanocatalyst [B20CuO76, B20Cu60, B18CuO61, and B18CuO65] on PCCI engine at 20, 40, 60, and 80% engine loads, respectively[59]. The 20% premixed percentage resulted in high in BTE, NO<sub>x</sub>, smoke opacity, and cylinder pressure with 14.08%, 58 ppm, 7%, and 51 bar for B20CuO76 at 20% load, 22.11%, 94 ppm, 12% and 54 bar for B20Cu60 at 40% load, 26.78%, 117 ppm, 14% and 57 bar for B18CuO61 at 60% load, and 23.39%, 130 ppm, 17% and 62 bar for B18CuO65 at 80% load, respectively. In contrast, there was a remarkable low in BSFC and CO, with 0.586 kg/kWh and 0.144% for B20CuO76 at 20% load, 0.367 kg/kWh and 0.135% for B20Cu60 at 40% load, 0.327 kg/kWh and 0.121% for B18CuO61 at 40% load, and 0.31 kg/kWh and 0.11% for B18CuO65 at 80% load, respectively. On the other hand, HC values had a diminishing effect at B20CuO76 at 20% load, B20Cu60 at 40% load, and B18CuO61 at 60% load with 70,

66, and 57 ppm, except for B18CuO65 at 80% load, which showed a considerable rise with 67 ppm.

The influences of performance and exhaust emissions parameters via the different blends of conventional diesel [97, 95, 92.5, and 90%] with various percentages of ammonium hydroxide [N2.5, N5, 7.5, and N10%] on PCCI engine were illustrated [60]. While ammonium hydroxide percentages were incremental, there was a considerable rise in the values of BTE, HC, and CO, whereas there was a noticeable decline in BSFC, EGT, NOx, and smoke emission as compared to conventional diesel [53, 60, 61].

This paper was explained in great detail about using ammonia as a fuel for premixed charge compression ignition engine [62]. Despite the obstacles in manufacturing, storage, and transportation, lowering carbon levels is a key priority for power generation and engine companies that work with zero-carbon sources like ammonia and hydrogen. One of the most significant study ideas with the aim of lowering carbon and other pollutants by making small adjustments to internal combustion engines is the use of one of the latest injection systems, such as premixed charge compression ignition and homogeneous charge compression ignition. Although ammonia is widely considered a viable substitute for conventional diesel fuel in applications that are not limited to large regions, like marine and heavy-duty applications, it's presently challenged by high levels of NOx emissions [62, 63]. This is because ammonia can be burned in the dual fuel system by injecting diesel into it. Further, the additional experimentation will have been performed lately about the utilisation of ammonia and the strategies to apply it within various engines of internal combustion modes because of its advantages of not having carbon atoms in it as well as the modern injection methods will be integrated with the research [64, 65].

The aim of this research is to study the effects of PCCI engine on engine characteristics such as performance, combustion, and exhaust emissions through an experiment when added to 1) various percentages of biodiesel and diesel blend and 2) various percentages of biodiesel and diesel blend with three different flow rates of HHO gas.

## II. THE EXPERIMENTAL METHODOLOGY AND PROCEDURE

### A. Experimental test setup

The operating machine schematic diagram as shown in the figure [1][53]. Figure [2] shows the back view of the operating machine, the driving motor, high-pressure pump, and premixing chamber are the three instruments that may be

seen next to each other at the bottom of the machine, respectively. Both the driving motor and high-pressure pump are located below the both return fuel tank [tank 2] and first pressure gauge regulator, whereas the three electric variac instruments and the vaporizer fuel control unit are placed above the both return fuel tank [tank 2] and first pressure gauge regulator. The air heater, air boiler, and temperature digital display, respectively, are all positioned above the premixing chamber, along with the exhaust gas recirculation [EGR] valve, exhaust valve, exhaust gas outlet, and exhaust tube. A second pressure gauge regulator can be found next to the air heater. The temperature digital display instrument is divided into three thermocouples of type K, including exhaust gases, a mixing chamber, and inlet air to monitor the temperature. Finally, they have an air tank on top of them, with a load panel in front of it.

Figure [3] shows the front view of the operating machine, there are three instruments beside each other at the bottom: a diesel [compression ignition] engine, a hydraulic dynamometer [generator], and a 3-phase electrical generator, as well as a CNG tank in front of the diesel engine. Above the diesel engine is an inclined manometer, alongside a fuel flow meter, graduated cylinders with stopcocks, respectively, and finally, an air tank on top of them. The first side view of the operating machine includes a side view of the vaporizer fuel control unit, air tank, load panel, diesel engine [compression ignition engine], driving motor, and return fuel tank [tank 2], as well as the front view of the load control unit, combustion analyzer data acquisition system, charge amplifier, and 3-phase variable transformer as shown in the figure [4][66]. The second side view of the operating machine will connect with the two exhaust measurement instruments: the exhaust gas analyzer and the smoke meter, by using each hose and inserting each hose of them into the exhaust gas outlet to record the exhaust emissions parameters as HC, CO, CO<sub>2</sub>, O<sub>2</sub>, and NOx emissions by the exhaust gas analyzer, but smoke opacity emissions by the smoke meter as shown in the figure [5].

The engine features a specialized electronic control unit [ECU] that adjusts the quantity of fuel pumped directly into the engine to maintain the engine speed at 1500 rpm. The operating machine had two fuel tanks[67]. The main tank [tank 1] is attached to a graduated cylinder to measure the amount of used fuel that is pumped directly to the engine per second, and the external tank [tank 2] is utilized to deliver the fuel to the external mixture. An eddy current dynamometer was used to load the engine. The dynamometer includes a 5 kW A.C. synchronous generator attached to the crank shaft, and the generator is linked to six lamps [each with 1 kW of power] and an electric voltage Variac instrument to adjust its output power [68-70].

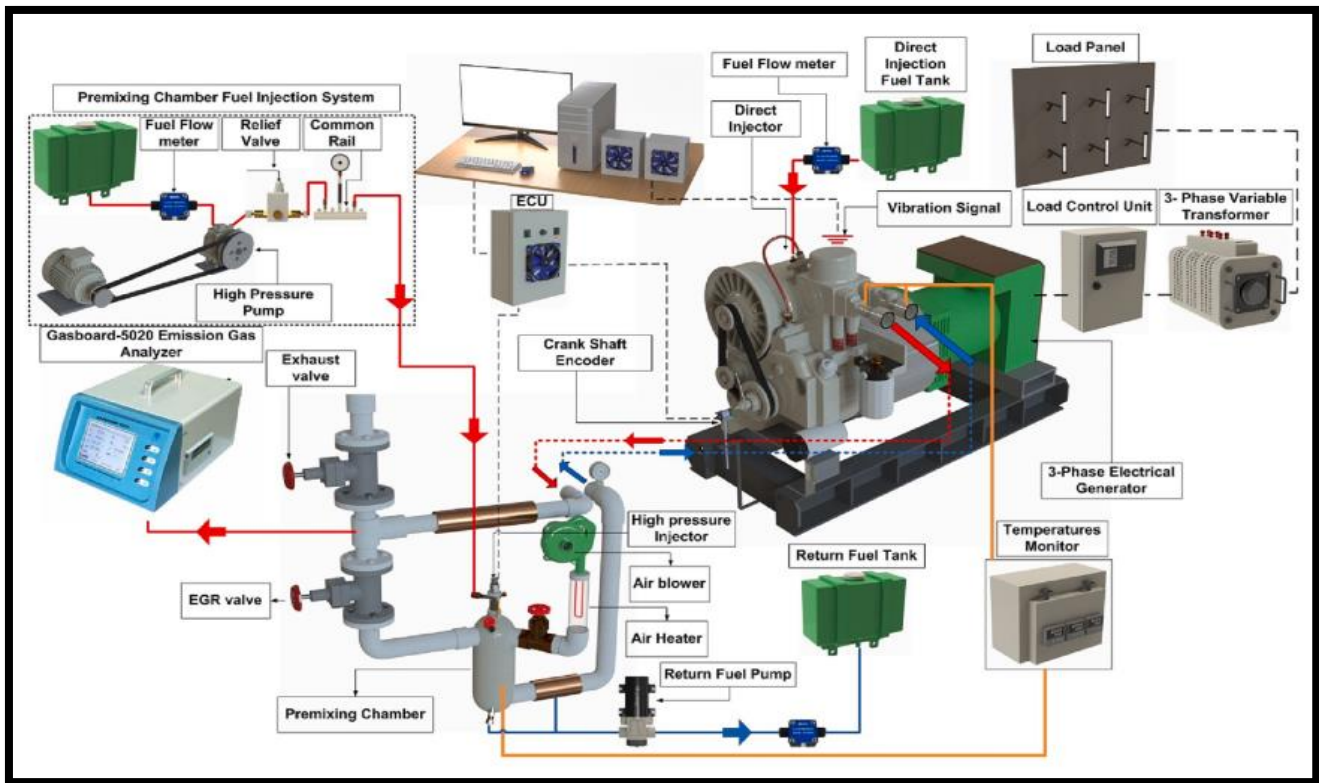


Figure 1: The operating machine schematic diagram [53].

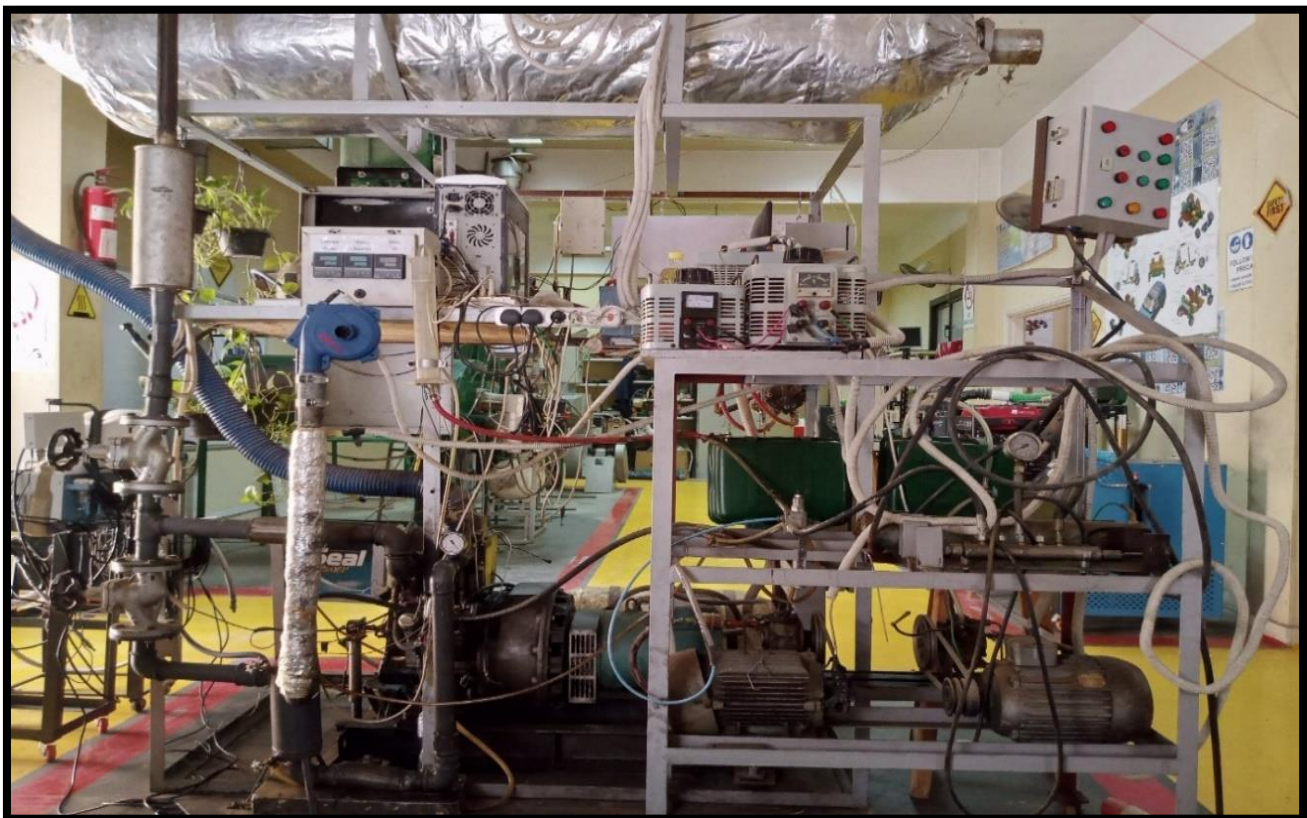


Figure 2: Back view of the operating machine.



Figure 3: Front view of the operating machine.



Figure 4: First side view of the operating machine.



Figure 5: Second side view of the operating machine.

A diesel [CI] engine that has been modified to function as a PCCI engine is used to investigate the operating characteristics of a PCCI engine that is fueled using a variety of blends of conventional diesel and biodiesel derived from sunflower and soybean oil. The diesel engine employed in this study has the following technical specifications: DEUTZ FL 511/W engine model, single cylinder, four strokes cycle, air-cooled system, direct injection mode, direct injection pressure fuel with 220 bar at a 32 CA before TDC, 10cm bore, 10.5 cm stroke, 825 cm<sup>3</sup>, 17 compression ratio, an operating rate power of 5 KW at 1500 rpm of constant speed, and 90 °C lubricating oil temperature. Further, the engine has an inlet valve that opens and closes at 32 °CA before TDC and 59 °CA after BDC, whereas the exhaust valve opens and closes at 71 °CA before BDC and 32 °CA after TDC, respectively. Table [1] lists the technical specifications of used engine.

Table 1: Technical specifications of diesel [CI] engine

Technical specifications of diesel [CI] engine	
Engine mode	DEUTZ FL 511/W
No. of Cylinders	Single cylinder
Cycle	Four strokes
Cooling System	Air Cooled
Bore	10 cm
Stroke	10.5 cm

Table 1: cont...

Technical specifications of diesel [CI] engine	
Displacement	825 cm <sup>3</sup>
Compression ratio	17
Rated Power	5 kW at 1500 rpm
Injection Mode	Direct injection
Inlet valve opens	32 °CA Before TDC
Inlet valve closes	59 °CA After BDC
Exhaust valve opens	71 °CA Before BDC
Exhaust valve closes	32 °CA After TDC
Direct injection pressure fuel	at 220 bar at a 32 CA Before TDC
Lubricating oil temperature	90 °C

### B. Measurements & Error analysis

In this study, the engine's crank shaft was installed with a speed sensor that recorded its speed. Three thermocouples of type K were used in a temperature digital display instrument that was divided into three sections: the inlet air, the exhaust gases, and the mixing chamber to record the temperature. Further, the inlet air part was positioned at the entrance of the air and the exhaust gases part was positioned at the outlet of exhaust emissions, while the mixing chamber part was used to

measure the temperature of the premixed mixture and was located between the inlet air and the exhaust gases. HC, CO<sub>2</sub>, CO, O<sub>2</sub>, and NO<sub>x</sub> readings were taken using the GASBOARD-5020 emission gas analyzer. While HC and NO<sub>x</sub> were measured by the measured unit of parts per million [ppm] and CO<sub>2</sub>, CO, and O<sub>2</sub> were determined by the measured unit of percentage volume [%Vol], on the other hand, smoke opacity [soot] emissions were recorded with a GASBOARD-6010 opacity meter by the measured unit of percentage volume [%Vol]. To measure various parameters, it requires several tools and equipment.

The accuracy of this equipment can be impacted by the working environment and conditions since it impacts the limiting measurement errors. In this investigation, the root-sum-squared [RSS] approach was employed to calculate the uncertainty of the errors' independent variables related to the observed values. The mean value and standard deviation of the data were estimated using Equations 1 and 2, respectively, which  $\bar{X}$  refer to the mean value,  $X_i$  refer to the variable's average [ $x$ ],  $n$  refer to the number of times the experiment may be repeated for measured data, and  $\sigma$  refer to the standard deviation, as well as equation 3 was used to compute the uncertainty equation for independent variables, which  $W_X$  refer to the uncertainty equation, meanwhile the overall uncertainty of dependent variable was showed in equation 4, which  $W_R$  refer to the overall uncertainty of dependent variable,  $R$  refer to the function uncertainty, and  $W_{X_1}, W_{X_2}, \dots, W_{X_n}$  refer to the independent variables uncertainties that represent the measured experimental operational factors  $X_1, X_2, \dots, X_n$  as shown below [4, 71-74].

$$\text{Eqn. ①: mean value: } \bar{X} = \frac{1}{n} * \sum_{i=1}^n X_i$$

$$\text{Eqn. ②: standarad deviation: } \sigma = \sqrt{\frac{1}{[n - 1]} * \sum_{i=1}^n [X_i - \bar{X}]^2}$$

$$\text{Eqn. ③: uncertainly equation: } W_X = \pm \frac{2 \sigma}{\bar{X}} * 100$$

$$\text{Eqn. ④: overall uncertainly: } W_R =$$

$$\sqrt{\left[\frac{\partial R}{\partial X_1} W_{X_1}\right]^2 + \left[\frac{\partial R}{\partial X_2} W_{X_2}\right]^2 + \dots + \left[\frac{\partial R}{\partial X_n} W_{X_n}\right]^2}$$

The accuracy and range of the exhaust gas analyzer instrument were  $\pm 5\%$  and 0-9999 ppm for HC,  $\pm 4\%$  and 0-20% for CO<sub>2</sub>,  $\pm 1\%$  and 0-20% for CO,  $\pm 3\%$  and 0-25% for O<sub>2</sub>, and  $\pm 5\%$  and 0-5000 ppm for NO<sub>x</sub>, as well as observed for the smoke meter instrument, which found  $\pm 0.01\%$  and 0-100% for smoke opacity. In addition, the accuracy and range recorded at the K-type thermocouple instrument were  $\pm 1\%$  and 0 to 800 °C to measure the

exhaust gas temperature parameter, and the speed by the shaft encoder instrument was observed at  $\pm 0.2\%$  for accuracy and 0–720 °CA for range. Inclined manometer, graduated cylinder/stopwatch, and load indicator instruments had an accuracy measurement of  $\pm 2\%$ ,  $\pm 1\%$ , and  $\pm 0.2\%$ , while the range measurement was 0–2.99 m<sup>3</sup>/h, 1 to 30 cm<sup>3</sup>, and 1 to 1000 W, which recorded the values of airflow rate, diesel flow meter, and load parameters, respectively. Table [2] shows the accuracy and range analysis for various types of equipment.

**Table 2: The accuracy and range analysis for various types of equipment**

Instrument	Parameters	Accuracy	Range
Exhaust gas analyzer	HC	$\pm 5\%$	0-9999 ppm
	CO <sub>2</sub>	$\pm 4\%$	0-20%
	CO	$\pm 1\%$	0-20%
	O <sub>2</sub>	$\pm 3\%$	0-25%
	NO <sub>x</sub>	$\pm 5\%$	0-5000 ppm
Smoke meter	Smoke opacity	$\pm 0.01\%$	0-100%
K-type thermocouple	Exhaust gas Temperature	$\pm 1\%$	0 to 800 °C
Shaft encoder	Speed	$\pm 0.2\%$	0–720 °CA
Inclined manometer	Airflow rate	$\pm 2\%$	0–2.99 m <sup>3</sup> /h
Graduated cylinder/stopwatch	Diesel flow meter	$\pm 1\%$	1 to 30 cm <sup>3</sup>
Load indicator	Load	$\pm 0.2\%$	1 to 1000 W

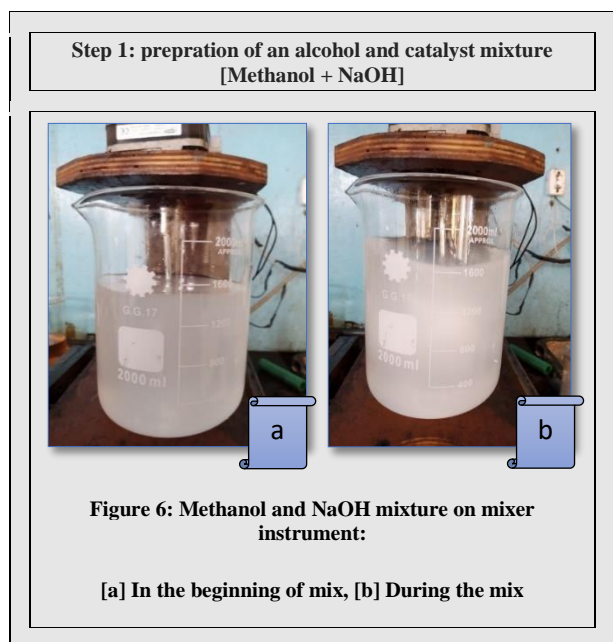
### C. Biodiesel production

#### C.1. Step 1. The alcohol and catalyst mixture are prepared as follows

The alcohol and catalyst mixture are prepared in the fuel laboratory at the Faculty of Engineering at Tanta University. Methanol is utilized as an alcohol that is purchased from laboratory chemicals, El-NAGAR for trading chemicals in Tanta, Egypt, while sodium hydroxide [NaOH] is used as a catalyst, which is bought from Tanta, Egypt, from Al-Pharaohs company for trade and import at laboratory chemicals. In the beginning, take a quantity of NaOH and weigh it on an electronic balance to estimate the weight required. For example, in this paper, we need 60 gm for every 6 liters of oil, then grind the parts of NaOH till they turn into a powder [for every 1 liter of oil, use 10 gm of NaOH, then for every 6 liters of oil, use 60 gm of NaOH]. After that, fill an empty beaker with 1500 milliliters, which is equal to 1.5 liters of methanol with 60 gm of NaOH [for every 1 liter of oil, use 250



milliliters [0.25 liters] of methanol, then for every 6 liters of oil, use 1500 milliliters [1.5 liters] of methanol]. Finally, place the beaker of NaOH with methanol mixtures on a mixer instrument for 10 minutes to obtain the mixture of alcohol and catalyst [NaOH + Methanol], as shown in figure [6].



### C.2. Step 2. The biodiesel is prepared as follows in two stages

Biodiesel is prepared at the fuel laboratory at the Faculty of Engineering at Tanta University. Table [3] contains the list of used components during the experiment, such as stirring machine components, electric heater, mixer instrument, electric kettle, 2 liters [2000 milliliters] beaker, and 1-liter [1000 milliliters] beaker. Use sunflower and soybean oil mixture in biodiesel production in two stages: 2.1. Separation process stage; 2.2. washing process stage by transesterification process. Moreover, the total quantity of usage oil is 12 liters, which is divided on the experiment into two phases, including the first phase for the first 6 liters and the second phase for the remaining 6 liters, while the washing process is done three times in phase 1 and twice in phase 2. Furthermore, the biodiesel yield is about 72.5%, which is a result of the sum of the biodiesel production quantities at phase 1 [4.2 liters] and phase 2 [4.5 liters], respectively, with the overall biodiesel production quantity equal to 8.7 liters as shown in the below sample calculation and table [6].

Total used oil = 12 liters, ①

1st six liters of biodiesel = 4.2 liters [phase 1],

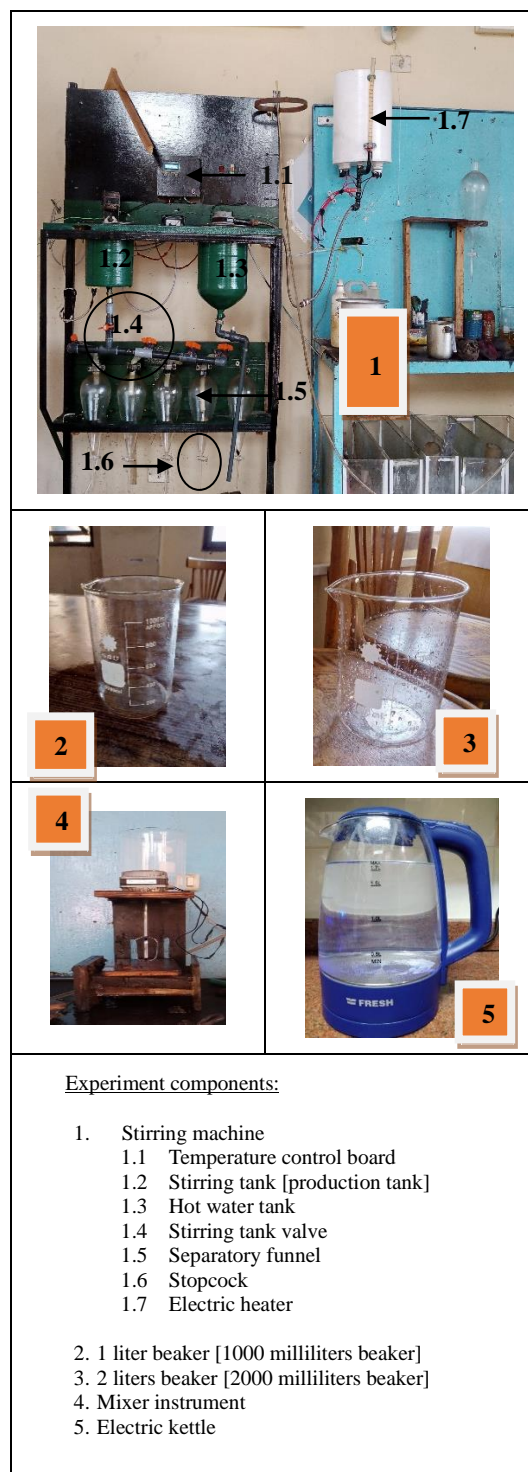
2nd remaining six liters of biodiesel = 4.5 liters [phase 2],

Overall biodiesel = 4.2 + 4.5 = 8.7 liters, ②

Then from ① and ②,

Biodiesel yield = 8.7 liters of total biodiesel / 12 liters of used oil =  $0.725 * 100 = 72.5\%$ . ③

**Table 3: Names of experimental items**



### C.2.1. Separation process stage

In a stirring tank, add 6 liters of sunflower and soybean oil mix, 1.5 liters of methanol, and 60 gm of NaOH. Then switch on the stirring machine at a temperature of 60 to 65 °C and a stirring speed of 500 to 700 rpm. After then, switch off the stirring machine, open the stirring machine valves, and close the stopcock of every separatory funnel to completely fill each separatory funnel with the output

mixture, then leave them for 24 hours as shown in table [4] for phases 1 and 2. After 24 hours, the output mixture [biodiesel and glycerin] forms three layers in the separatory funnel [top layer, middle layer, and bottom layer]. The top layer is biodiesel oil, the middle layer is biodiesel plus glycerin blend, and the bottom layer is glycerin, as shown in table [4] for phases 1 and 2. This is the time to prepare for the first stage of the separation process, which separates biodiesel oil and glycerin. Open the separatory funnel stopcock until the glycerin layer is removed into the 20-liters plastic jerry can, then close it to keep the biodiesel oil layer in the separatory funnel, as well as repeat it for the other remaining separatory funnels. Now, open the stopcock of the separatory funnel to collect a pure biodiesel oil layer free of glycerin in a sterile 20-liters plastic jerry can. Finally, once the separating process stage is complete, the next stage will begin, which is called the washing process stage.

**C.2.2. washing process stage**

The washing process stage is the following step after the separation process stage. The goal of the washing process

stage is to clean up the generated biodiesel from any impurities, dirt, and unresolved fatty acid residues via water at a specific temperature and mixing conditions. Boil the water to a temperature of 100°C in an electric kettle. Fill an empty beaker with 1 liter of hot water plus 1 liter of biodiesel from a sterile 20-liters plastic jerry can, then set them on the mixer instrument for 30 seconds. Repeat this procedure for every 1 liter of biodiesel from a sterile 20-liters plastic jerry can and add 1 liter of hot water to it until the output production amount of biodiesel is finished. The washing steps are repeated several times till the lower layer becomes like water color, which is only done three times for phase 1 and twice times for phase 2 in this paper, as shown in table [5] for phase 1 and phase 2. Finally, at the end of each phase, the biodiesel manufacturing outputs will be mixed with a chemical product known as calcium chloride dihydrate extra pure. Table [6] demonstrate the value of biodiesel produced, which is 4.2 liters and 4.5 liters, respectively, so the total quantity of biodiesel produced is equal to 8.7 liters.

**Table 4: Separation process at phase1 and phase 2**

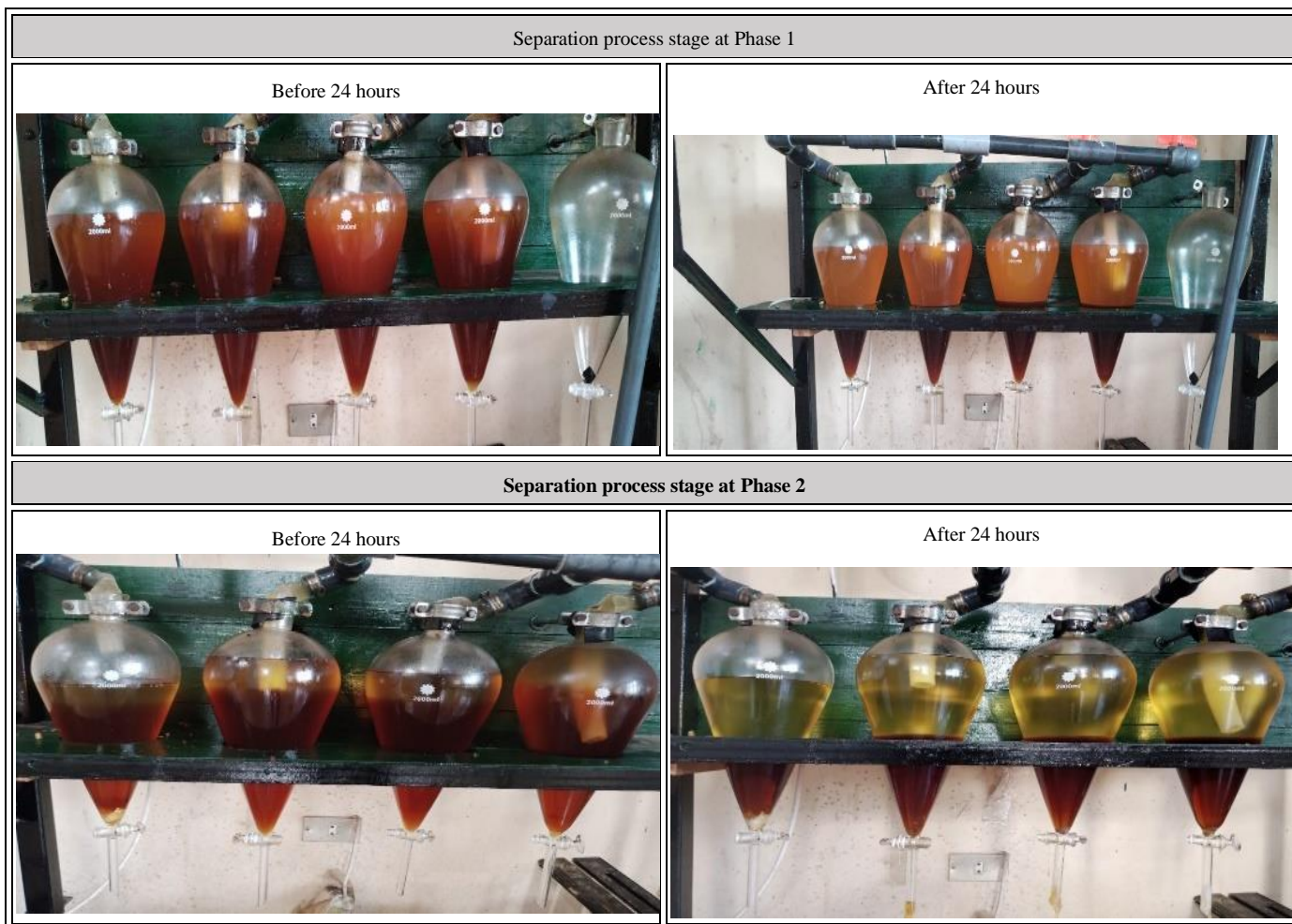





Table 5: Washing process stage for phase 1 and phase 2

I. Biodiesel plus hot water on mixer instrument			
			
2.The three times of biodiesel washing process stage at phase 1			
[2.1] 1 <sup>st</sup> time	[2.2] 2 <sup>nd</sup> time	[2.3] 3 <sup>rd</sup> time	
			
			
3. The two times of biodiesel washing process stage at phase 2			
[3.1] 1 <sup>st</sup> time		[3.2] 2 <sup>nd</sup> time	
			

Table 6: Biodiesel yields at phase 1 and phase 2

Phase1: first 6 liters biodiesel yield [4.5 liters]	Phase 2: second 6 liters biodiesel yield [4.2 liters]	Total = 8.7 liters
		

**C.3. Step 3: Prepare four various biodiesel and diesel blends**

After the biodiesel manufacturing process is completed, the preparation of biodiesel and diesel blends will begin in this paper. Furthermore, employ a variety of biodiesel and diesel percentages mixed, such as 20% biodiesel plus 80% diesel, 40% biodiesel plus 60% diesel, 60% biodiesel plus 40% diesel, and 80% biodiesel plus 20% diesel. Fill an empty 1 liter [1000 milliliters] beaker with an experimental concentration of biodiesel and diesel blend, then transfer the blend to an empty 2 liters [2000 milliliters] beaker to ensure that the blend does not come out of the beaker during the mixing process, and finally set it on the mixer instrument for 1 hour to create the blend. The above steps should be repeated for each concentration. The outcomes of blends are clarified further in figure [7].



Figure 7: Four biodiesel/diesel blends.

**C.4. Step 4: Prepare the blend of 40% biodiesel plus 60% diesel again**

The mix of 40% biodiesel and 60% diesel was chosen to be prepared again for addition to the HHO gas instrument to acquire the result of concentration with the effect of HHO gas. To obtain the blend, fill an empty 1 liter [1000 milliliters] beaker with 40% biodiesel and 60% diesel, then transfer it to an empty 2 liters [2000 milliliters] beaker and place it on the mixer instrument for 1 hour.

This step should be done four times to output 4 liters of a 40% biodiesel and 60% diesel blend, as shown in figure [8].

**C.5. Step 5: Introduction before starting work on the PCCI engine machine**

After completing steps 3 and 4, proceed to the internal combustion laboratory to begin the paper's research on PCCI engine characteristics such as performance, combustion, and exhaust emissions by using eight various blends, including conventional diesel only, four blends of biodiesel and diesel mix, and three concentrations of HHO gas with the addition of 40% biodiesel and 60% diesel blend. Further, all usage fuels or blends are listed in table [7].

Table 7: Used fuel/blend names

Used fuel/blend names	Abbreviations
conventional diesel	D100
20% biodiesel and 80% diesel blend	B20D80
40% biodiesel and 60% diesel blend	B40D60
60% biodiesel and 40% diesel blend	B60D40
80% biodiesel and 20% diesel blend	B80D20
40% biodiesel and 60% diesel blend + HHO [5 LPM]	B40D60 + HHO [5 LPM]
40% biodiesel and 60% diesel blend + HHO [10 LPM]	B40D60 + HHO [10 LPM]
40% biodiesel and 60% diesel blend + HHO [15 LPM]	B40D60 + HHO [15 LPM]

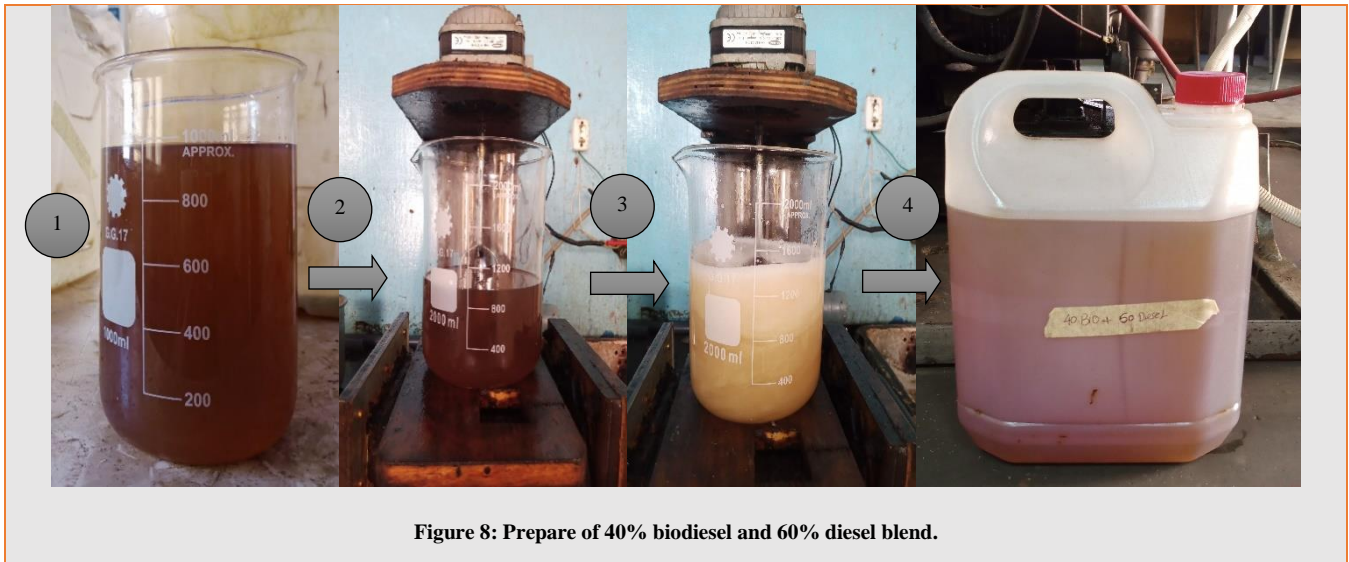


Figure 8: Prepare of 40% biodiesel and 60% diesel blend.

### III. RESULTS AND DISCUSSION

#### A. Engine performance analysis

In the first section shows the performance of engine such as BTE, BSFC, and EGT by the experimental of eight blends in PCCI engine.

##### 1. Brake thermal efficiency [BTE]

BTE is the relationship between the power output of the brake shaft and the rate at which the fuel's thermal energy is consumed[75]. The relationship between BTE and engine brake power is directly proportional. The low heat loss in all experimental cases and the boost in output power owing to improved combustion quality led to a rise in BTE as the engine brake power increased. To determine the brake thermal efficiency value, use the form below.

$$\text{BTE [\%]} = \left[ \frac{\text{The power produced in kilowatt [kw]}}{\left[ \frac{\text{The fuel consumption rate in grams per second [g/sec.]} * 42600 \right]} \right] * 10^5$$

The highest BTE is at 3.4866 KW with 26.8% of D100, but the lowest BTE is at 0.671775 with 8.5% of B60D40; therefore, both B20D80 and B40D60 blends have higher BTE values than conventional diesel fuel, whereas D100 is higher than B60D40 and B80D20. As biodiesel concentration increases, BTE recorder values decrease, owing to the fact that biodiesel has a lesser calorific value and a greater viscosity, density, and surface tension as compared to conventional diesel fuel. This results in low atomization and air mixing, resulting in poor combustion and minimal BTE.

Moreover, when HHO gas is added to 40% biodiesel and diesel blend with flow rates of 5, 10, and 15 LPM, there is a remarkable increase in BTE, due to the large

heating value and fast flame speed of HHO. The figures [9] and [10], which illustrate the findings with a simple graph that represents the noticeable increases in brake thermal efficiency for all test conditions.

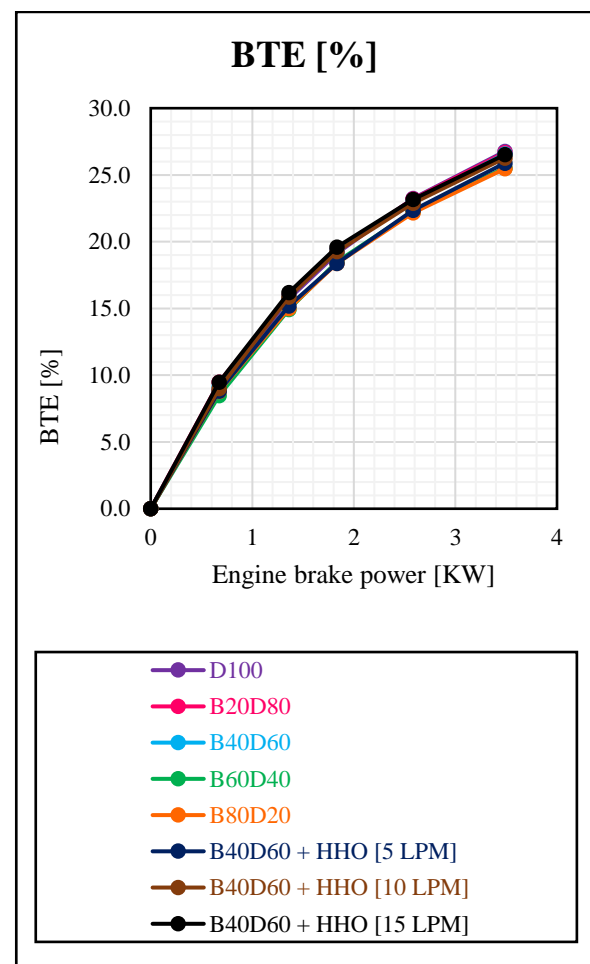


Figure 9: BTE values vs Engine brake power.

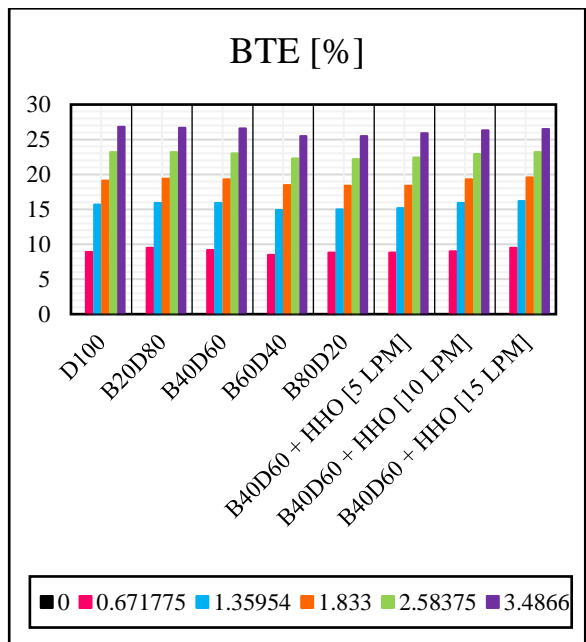


Figure 10: BTE values vs Engine brake power.

2. Brake specific fuel consumption [BSFC]

It is a gauge of a prime mover's fuel efficiency when it burns fuel to generate rotational or shaft power[75]. The relationship between BTE and BSFC is inversely proportional, so if the relation between BSFC and engine brake power is inversely proportional, then BSFC decreases as engine brake power increases owing to improved combustion quality and increased energy controllability. To determine the brake specific fuel consumption values, use the form below.

$$BSFC [g/kw.hr] = \frac{\text{The fuel consumption rate in grams per second [g/sec.]} \times 3600}{\text{The power produced in kilowatt [kw]}}$$

The highest BSFC is at 0.671775 KW with 996 g/kw.hr of B60D40, but the lowest BSFC is at 3.4866 with 316 g/kw.hr of D100; therefore, both B20D80 and B40D60 blends have lesser BSFC values than conventional diesel fuel, whereas D100 is higher than B60D40 and B80D20. As biodiesel concentration increases, BSFC recorder values increase, except for the B80D20 blend, which has unstable values because of the lesser heating fuel of biodiesel fuel and its greater viscosity, low spray generation occurs, resulting in poor combustion quality.

Moreover, when HHO gas is added to 40% biodiesel and diesel blend with flow rates of 5, 10, and 15 LPM, there is a remarkable lower BSFC record than both conventional diesel fuel and various biodiesel/diesel blends. HHO improves full combustion due to its elevated flame speed and high octane rating. Further, the use of HHO gas improves combustion efficiency, especially at

high speeds when bio-fuel blends are difficult to totally burn due to greater residual gas and a lack of mixing in lean cases. Figures [11] and [12] illustrate the findings with a simple graph that represents the noticeable decreases in brake specific fuel consumption for all test conditions.

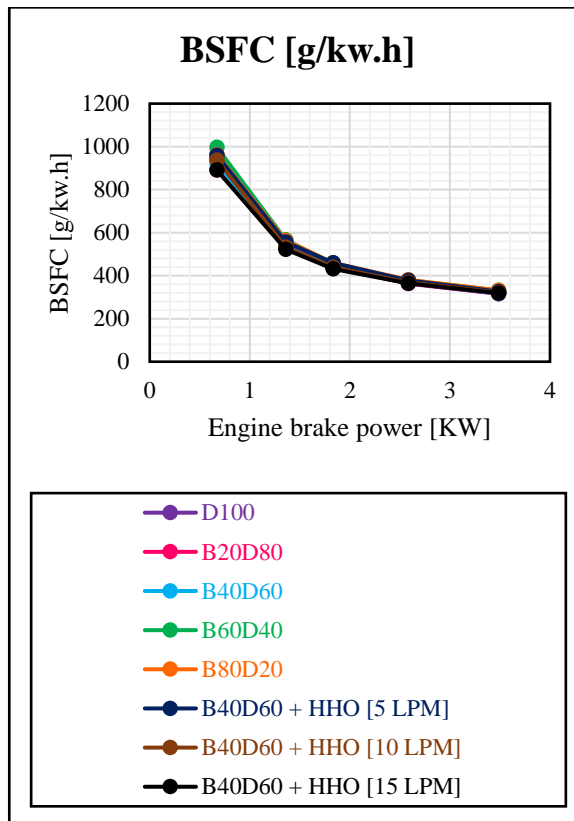


Figure 11: BSFC values vs Engine brake power.

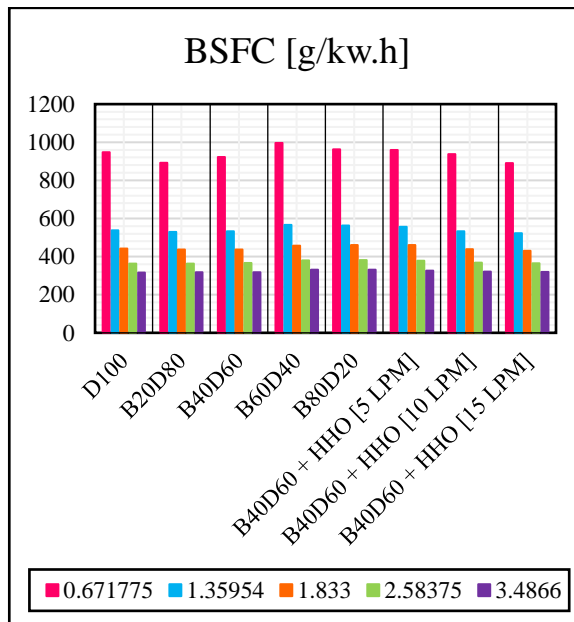


Figure 12: BSFC values vs Engine brake power.

### 3. Exhaust gas temperature [EGT]

It is a temperature measurement recorded at the engine's back end[34]. The relationship between EGT and engine brake power is directly proportional, so EGT increases as engine brake power increases because of increased consumption of fuel, which raises energy release as a result of a greater rate of combustion.

The highest EGT is at 3.4866 KW with 311 °C of D100, but the lowest EGT is at zero Kw with 106 °C of B40D60 + HHO [15 LPM]; therefore, the various biodiesel blends have lesser EGT values than conventional diesel fuel. As biodiesel concentration increases, EGT recorder values decrease due to the fact that biodiesel has a smaller heating value and a greater viscosity value.

Moreover, when HHO gas is added to 40% biodiesel and diesel blend with flow rates of 5, 10, and 15 LPM, there is a remarkable lower EGT record than both conventional diesel fuel and various biodiesel/diesel blends.

Figures [13] and [14] illustrate the findings with a simple graph that represents the noticeable increases in exhaust gas temperature for all test conditions.

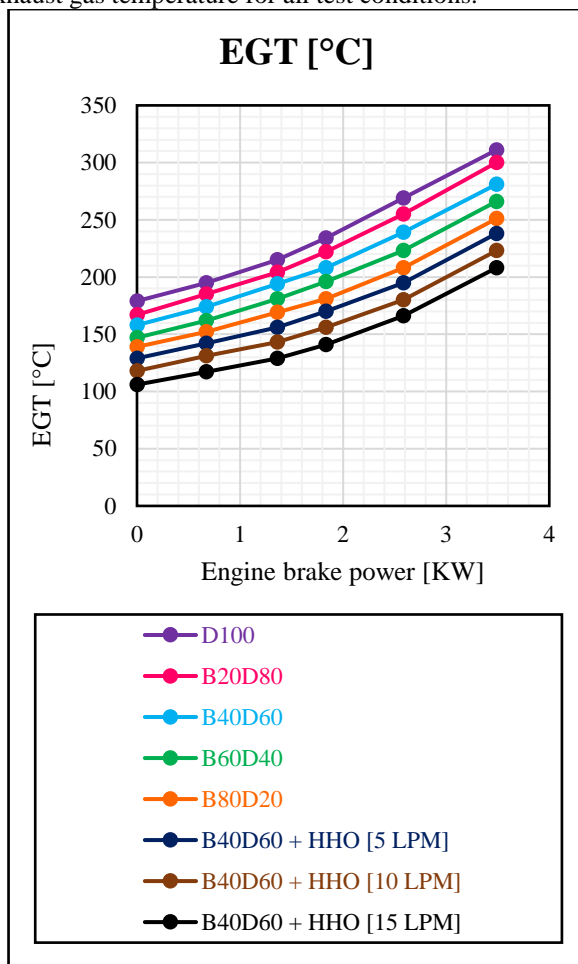


Figure 13: EGT values vs Engine brake power.

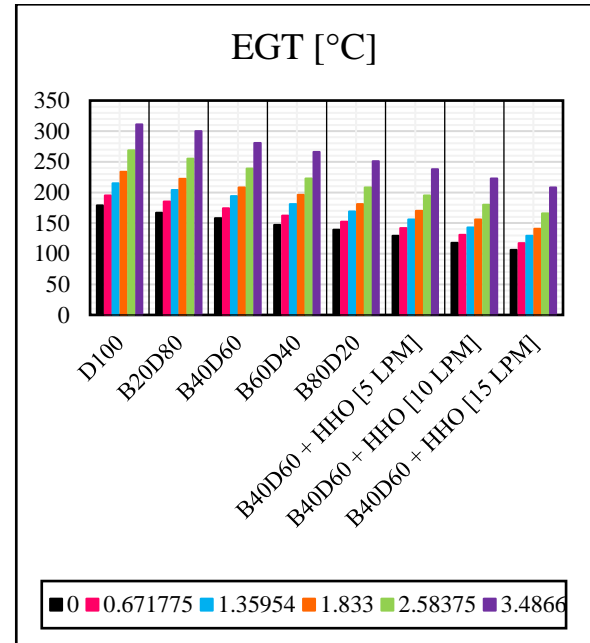


Figure 14: EGT values vs Engine brake power.

### B. Engine exhaust emissions analysis

In the second section illustrates the levels of exhaust emission [as: HC, CO, CO<sub>2</sub>, O<sub>2</sub>, NO<sub>x</sub>, and SOOT] that get out from experimental for eight blends in PCCI engine.

#### 1. Hydrocarbon [HC]

Hydrocarbon emissions are created as the outcome of incomplete combustion of the fuel confined in the slit volumes, a mixture that is either extremely lean or excessively rich, and wetting of the liquid wall. Additionally, the two most common contributing factors to HC emissions are the incomplete evaporation of fuel and a small distance to extinguish the flame[75]. The relationship between HC and engine brake power is directly proportional, so HC increases as engine brake power increases because of the full combustion, which enhances both combustion temperature and efficiency.

At 3.4866 KW, there is the highest HC with 36 PPM of D100, but the lowest HC is at zero Kw with 8 PPM of B40D60 + HHO [15 LPM]; therefore, the various biodiesel blends have lesser HC values than conventional diesel fuel. As biodiesel concentration increases, CO recorder values decrease due to full combustion that occurs from the oxygen content of biodiesel blends.

Moreover, when HHO gas is added to 40% biodiesel and diesel blend with flow rates of 5, 10, and 15 LPM, there is a remarkable lower CO record than both conventional diesel fuel and various biodiesel/diesel blends due to more diffusivity and minimal igniting energy. The hydrocarbon oxidation occurred as a result of the existence of hydrogen and oxygen atoms in the experimental fuel when hydrogen was added to the system. Figures [15] and [16] illustrate the findings with a

simple graph that represents the noticeable increases in hydrocarbon emissions for all test conditions.

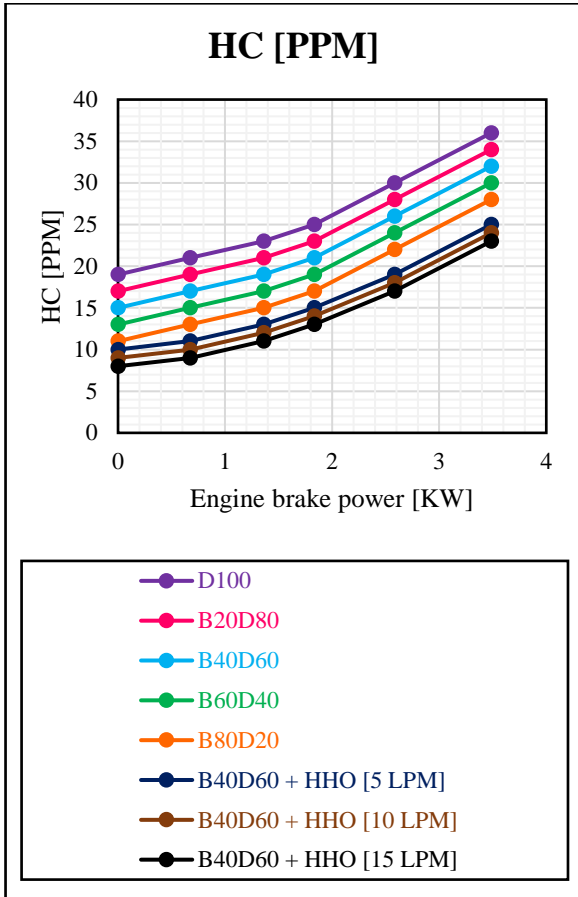


Figure 15: HC values vs Engine brake power.

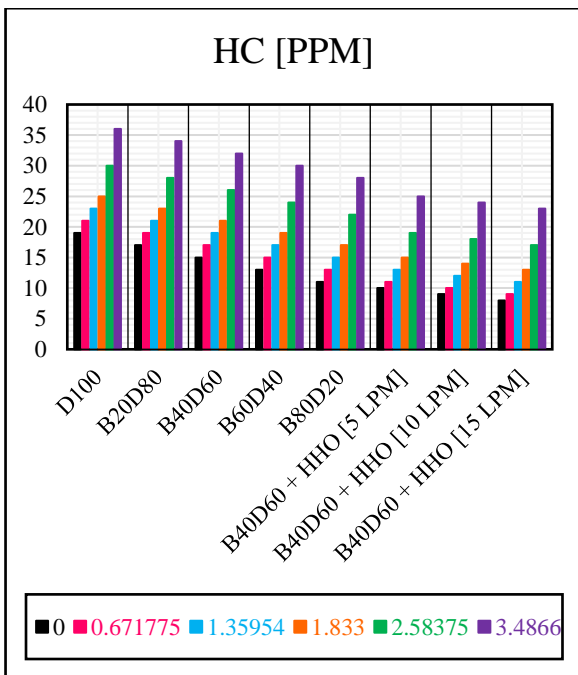


Figure 16: HC values vs Engine brake power.

## 2. Carbon dioxide [CO<sub>2</sub>]

Once all of the carbon that exists in the fuel is fully burned, carbon dioxide emissions are produced. The conversion of oxygen molecules results in a decrease in CO<sub>2</sub> production when CO levels rise. The carbon balancing phenomenon is used to improve the generation of CO and CO<sub>2</sub> in exhaust gases[75]. The relationship between CO<sub>2</sub> and engine brake power is directly proportional, so CO<sub>2</sub> increases as engine brake power increases owing to the elevated rate of full combustion.

At 3.4866 KW, there is the highest CO<sub>2</sub> with 5.77% of D100, but the lowest CO<sub>2</sub> is at zero Kw with 1.02% of B40D60 + HHO [15 LPM]; therefore, the various biodiesel blends have lesser CO<sub>2</sub> values than conventional diesel fuel. As biodiesel concentration increases, CO<sub>2</sub> recorder values decrease because biodiesel has a greater H/C ratio and blends of biodiesel do not combust completely.

Moreover, when HHO gas is added to 40% biodiesel and diesel blend with flow rates of 5, 10, and 15 LPM, there is a remarkable lower CO<sub>2</sub> record than both conventional diesel fuel and various biodiesel/diesel blends due to the fact that HHO does not contain any carbon and the presence of oxygen and hydrogen in HHO boosts combustion.

Figures [17] and [18] illustrate the findings with a simple graph that represents the noticeable increases in carbon dioxide emissions for all test conditions.

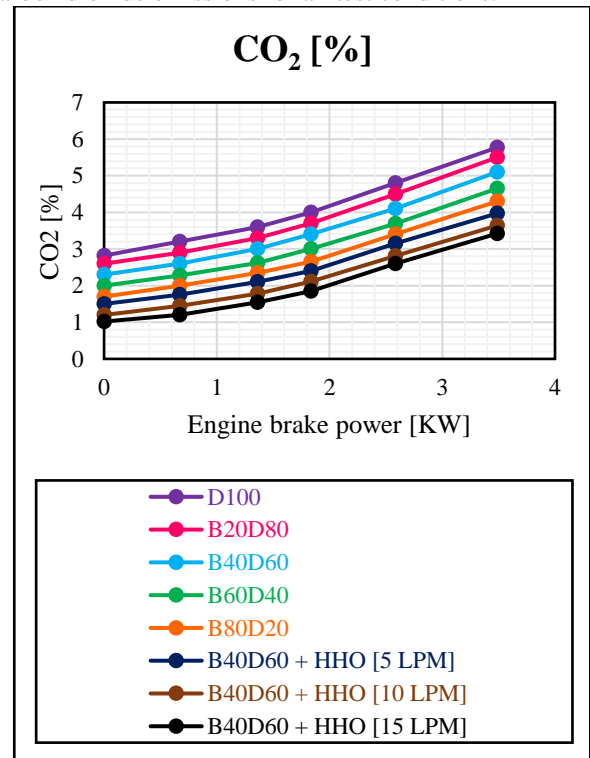
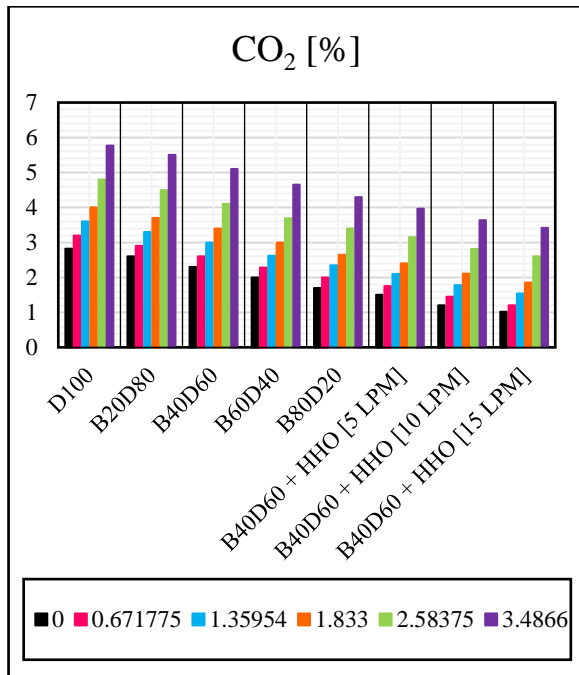


Figure 17: CO<sub>2</sub> values vs Engine brake power.



Figure 18: CO<sub>2</sub> values vs Engine brake power.

### 3. Carbon monoxide [CO]

CO is produced in the cylinders at uncomplete combustion and an overabundance of fuel; likewise, the creation of CO results from a rich fuel combination and not enough quantity of oxygen in the fuel. The CO level is determined by uncompleted combustion, which results in a partial oxidation of carbon owing to poor combustion temperature and an absence of oxygen[75]. The relationship between CO and engine brake power is directly proportional, so CO increases as engine brake power increases because the temperature of combustion rises and combustion time becomes smaller.

At 3.4866 KW, there is the highest CO with 0.53% of D100, but the lowest CO is at zero Kw with 0.03% of B40D60 + HHO [15 LPM]; therefore, the various biodiesel blends have lesser CO values than conventional diesel fuel. As biodiesel concentration increases, CO recorder values decrease due to full combustion that occurs from the oxygen content of biodiesel blends.

Moreover, when HHO gas is added to 40% biodiesel and diesel blend with flow rates of 5, 10, and 15 LPM, there is a remarkable lower CO record than both conventional diesel fuel and various biodiesel/diesel blends because of the high air/fuel mix.

Figures [19] and [20] illustrate the findings with a simple graph that represents the noticeable increases in carbon monoxide emissions for all test conditions.

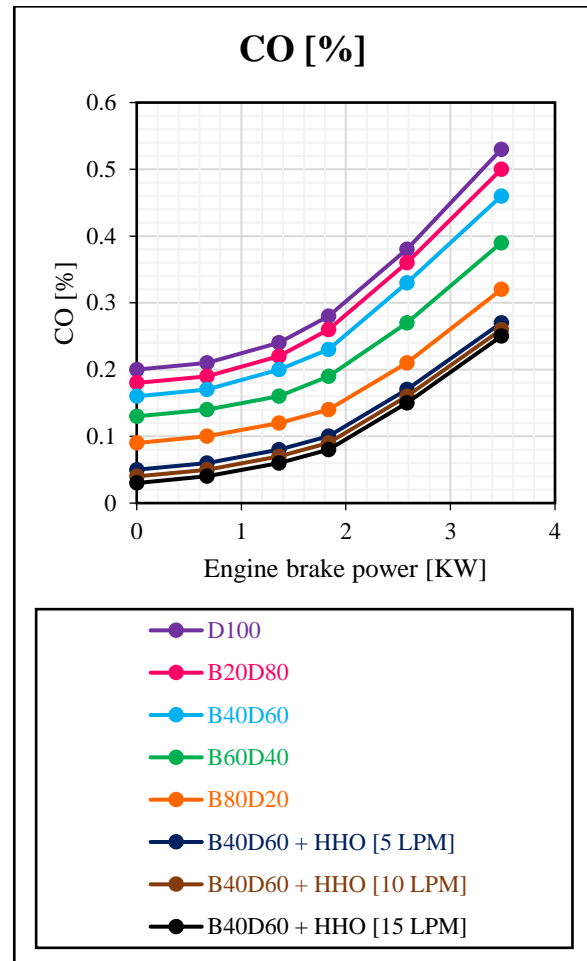


Figure 19: CO values vs Engine brake power.

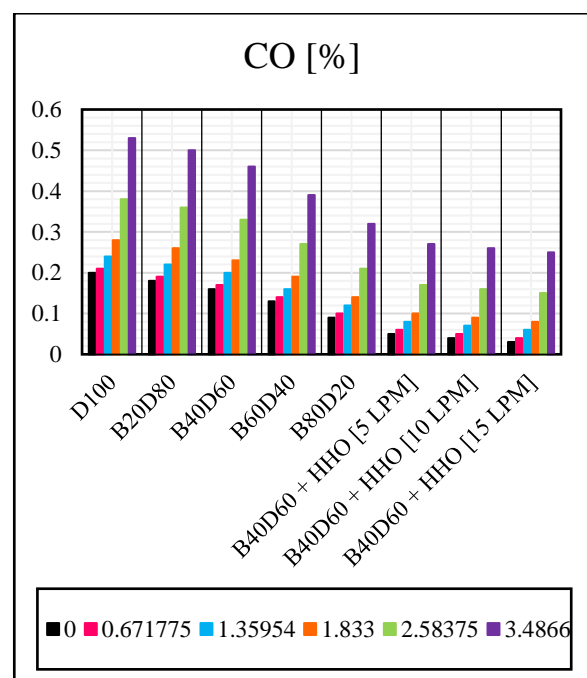


Figure 20: CO values vs Engine brake power.

4. Oxygen rate [O<sub>2</sub>]

Oxygen rate is the quantity of oxygen that remains when there is no combustion. Additionally, while there is an overabundance of air in the mixture, free O<sub>2</sub> is formed in the exhaust[75]. The relationship between O<sub>2</sub> and engine brake power is inversely proportional, so O<sub>2</sub> decreases as engine brake power increases owing to more fuel being supplied and more oxygen being needed for combustion to be performed. At zero KW, there is the highest O<sub>2</sub> with 18.8% of D100, but the lowest O<sub>2</sub> is at 3.4866 Kw with 11.13% of B40D60 + HHO [15 LPM]; therefore, the various biodiesel blends have lesser O<sub>2</sub> values than conventional diesel fuel. As biodiesel concentration increases, O<sub>2</sub> recorder values decrease because of incomplete fuel combustion, exhaust system, and infiltration in the manifold.

Moreover, when HHO gas is added to 40% biodiesel and diesel blend with flow rates of 5, 10, and 15 LPM, there is a remarkable lower O<sub>2</sub> record than both conventional diesel fuel and various biodiesel/diesel blends. Figures [21] and [22] illustrate the findings with a simple graph that represents the noticeable decreases in oxygen rate emissions for all test conditions.

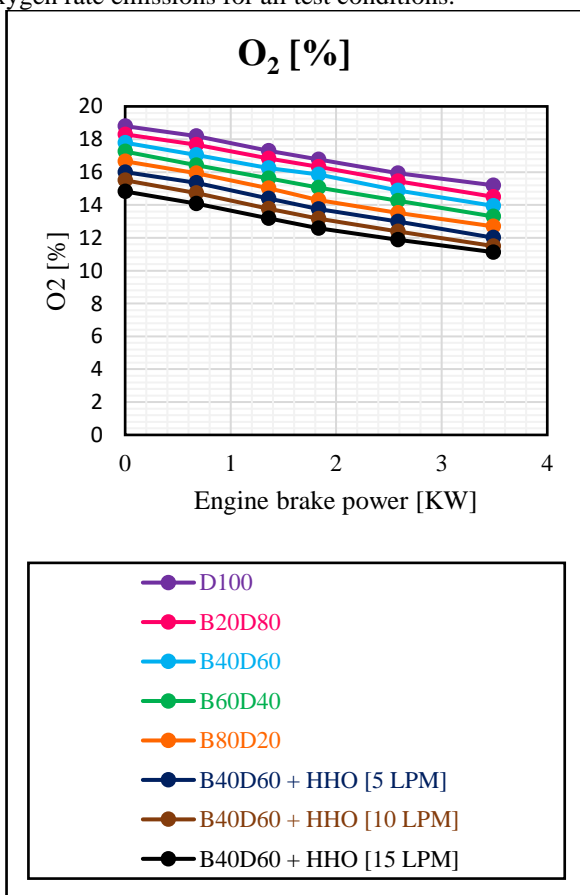


Figure 21: O<sub>2</sub> values vs Engine brake power.

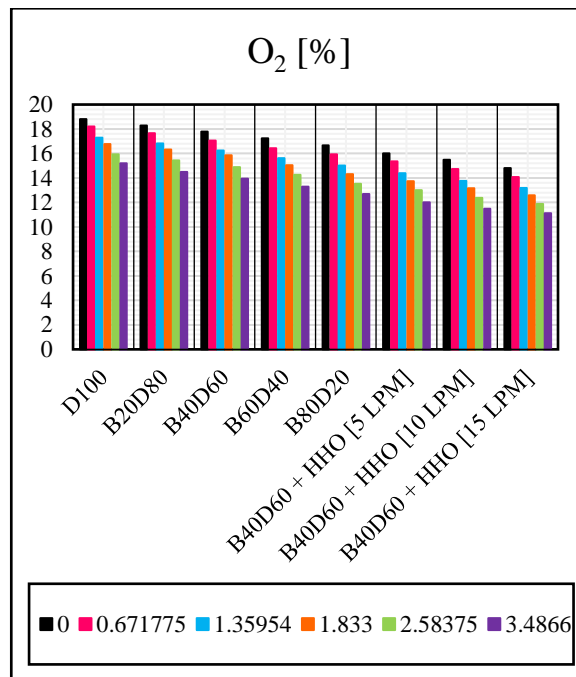


Figure 22: O<sub>2</sub> values vs Engine brake power.

5. Nitrogen oxide [NO<sub>x</sub>]

Both nitric oxide [NO] and nitrogen dioxide [NO<sub>2</sub>] are the two major components of nitrogen oxide [NO<sub>x</sub>], which are hazardous for humans, the ecosystem [as acid rain, smog, and ground-level ozone generation], and limiting engine development. The higher amount of oxygen available, the rising temperature of the combustion chamber, and the longer the combustion residence duration are the factors that affect NO<sub>x</sub> levels. So, the better the combustion quality and the higher the temperature, that cause more NO<sub>x</sub> to be generated[75]. The relationship between NO<sub>x</sub> and engine brake power is directly proportional, so NO<sub>x</sub> increases as engine brake power increases due to raising the temperature of the combustion chamber.

At 3.4866 KW, there is the highest NO<sub>x</sub> with 725 PPM of D100, but the lowest NO<sub>x</sub> is at zero Kw with 97 PPM of B40D60 + HHO [15 LPM]; therefore, the various biodiesel blends have lesser NO<sub>x</sub> values than conventional diesel fuel. As biodiesel concentration increases, NO<sub>x</sub> recorder values decrease because biodiesel blends include more oxygen concentration, they have a leaner air-fuel combination, which accelerates the interaction between oxygen and nitrogen, resulting in NO<sub>x</sub> emissions.

Moreover, when HHO gas is added to 40% biodiesel and diesel blend with flow rates of 5, 10, and 15 LPM, there is a remarkable lower NO<sub>x</sub> record than both conventional diesel fuel and various biodiesel/diesel blends because of the oxygen content of the fuel.

Figures [23] and [24] illustrate the findings with a simple graph that represents the noticeable increases in nitrogen oxide emissions for all test conditions.

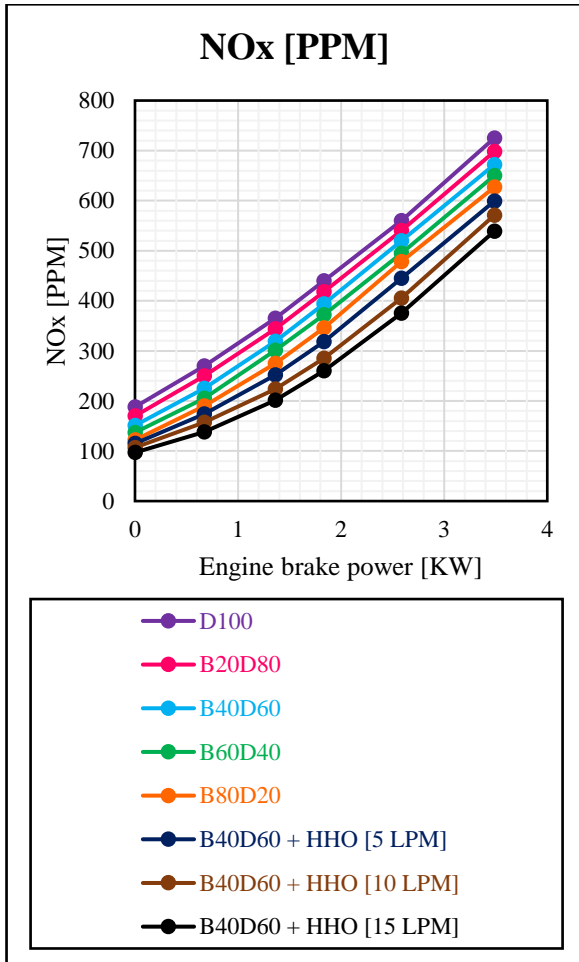


Figure 23: NOx values vs Engine brake power.

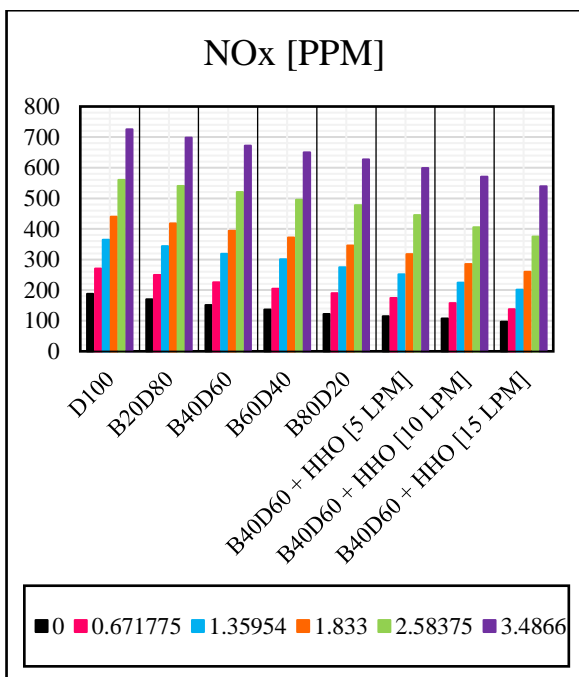


Figure 24: NOx values vs Engine brake power.

### 6. Smoke intensity [Soot]

Smoke intensity means a pollutant generated by combustion in a flare and occurring immediately downstream of the flame[34]. The relationship between soot and engine brake power is directly proportional, so soot increases as engine brake power increases owing to incomplete combustion, this happens at high loads because there is an injection of high fuel, resulting in increased smoke levels. At 3.4866 KW, there is the highest soot with 86.9% of D100, but the lowest soot is at zero Kw with 2% of B40D60 + HHO [15 LPM]; therefore, the various biodiesel blends have lesser soot values than conventional diesel fuel. As biodiesel concentration increases, soot recorder values decrease because biodiesel has a greater viscosity and more cetane number, which reduces the possibility of fuel-rich zones forming. Also, biodiesel-based fuels have more oxygen and less carbon than diesel fuel. Moreover, when HHO gas is added to 40% biodiesel and diesel blend with flow rates of 5, 10, and 15 LPM, there is a remarkable lower soot record than both conventional diesel fuel and various biodiesel/diesel blends because the addition of the hydroxyl raises the oxygen content, hence improving full combustion.

Figures [25] and [26] illustrate the findings with a simple graph that represents the noticeable increases in smoke intensity [soot] emissions for all test conditions.

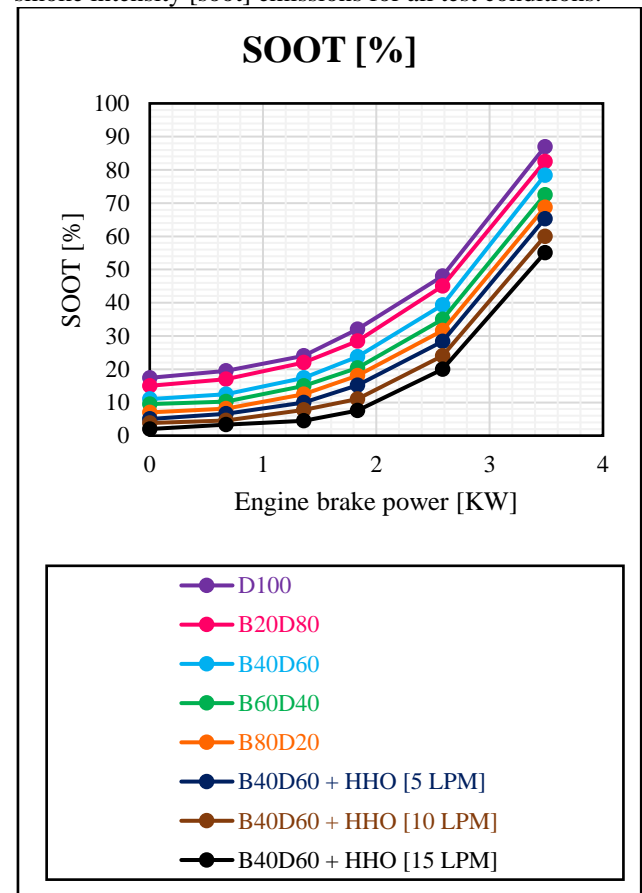


Figure 25: Soot values vs Engine brake power.

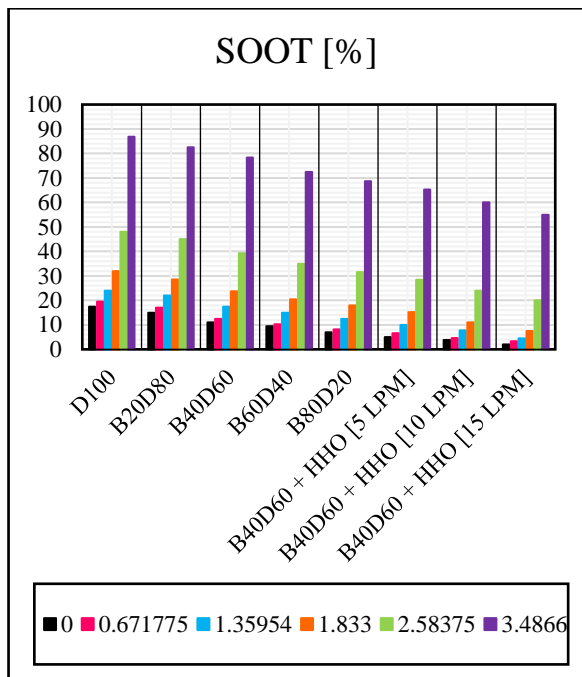


Figure 26: Soot values vs Engine brake power.

C. Weighted Average

The weighted average findings will be discussed below, as well as the outcomes that will be compared between conventional diesel fuel, various biodiesel and diesel blends, and oxyhydrogen gas with a B40D60 blend, to obtain an ideal mixing ratio with which we may later work and incorporate into future studies. The weighted average results will be estimated via the following equation:

$$W = \frac{\sum_{i=1}^n [\omega_i * X_i]}{\sum_{i=1}^n \omega_i}$$

where W refers to weight average, n refers to the number of terms to be averaged,  $\omega_i$  refers to weights applied to x values, and  $X_i$  refers to data values to be averaged.

1. Weighted average of performance characteristics

1.1 Weighted average of BTE

As shown in the figure [27], the most weighted average value of BTE at B40D60 + HHO [15 LPM] is 21.8%, whereas the least value is found with 20.7% of B80D20 as compared to other used mixtures, so the 40% biodiesel and diesel blend plus oxyhydrogen gas with a flow rate of 15 LPM is the best weighted average record to use. As various biodiesel and diesel blends rise, the weighted averages of BTE drop. In contrast, if HHO gas flow rates increase and are then added to the B40D60 blend, it results in a considerable increment in BTE values. While the BTE records the value of conventional diesel fuel by 21.72%, which is lower than B20D80 and B40D60 + HHO [15 LPM] but higher than all remaining other test blends.

1.2 Weighted average of BSFC

As shown in the figure [28], the most weighted average value of BSFC at B60D40 is 444.1536677 g/kw.h, whereas the least value is found with 417.7914504 g/kw.h of B40D60 + HHO [15 LPM] as compared to other used mixtures, so the 40% biodiesel and diesel blend plus oxyhydrogen gas with a flow rate of 15 LPM is the best weighted average record to use. As various biodiesel and diesel blends rise, the weighted averages of BSFC increase, except for the blend B80D20, which is less by 442.7057058 g/kw.h than B60D40. In contrast, if HHO gas flow rates increase and are then added to the B40D60 blend, it results in a considerable reduction in BSFC values. While the BSFC records the value of conventional diesel fuel at 424.4661904 g/kw.h, which is higher than B20D80, B40D60, and B40D60 + HHO [15 LPM] but lower than all remaining other test blends.

1.3 Weighted average of EGT

As shown in the figure [29], the most weighted average value of EGT at D100 is 264.9 °C, whereas the least value is found with 167.8 °C of B40D60 + HHO [15 LPM] as compared to other used mixtures, so conventional diesel fuel is the best weighted average record to use. Furthermore, B20D80 outcomes are better than all oxyhydrogen results using three flow rates [5, 10, and 15 LPM] when added to a 40% biodiesel and diesel blend at 253 °C. As various biodiesel and diesel blends rise, the weighted averages of EGT drop. On the other hand, if HHO gas flow rates increase and are then added to the B40D60 blend, it results in a considerable reduction in EGT values.

2. Weighted average of exhaust emissions characteristics

2.1 Weighted average of HC

As shown in the figure [30], the most weighted average value of HC at D100 is 29.62 PPM, whereas the least value is found with 17.01 PPM of B40D60 + HHO [15 LPM] as compared to other used mixtures, so the 40% biodiesel and diesel blend plus oxyhydrogen gas with a flow rate of 15 LPM is the best weighted average record to use. As various biodiesel and diesel blends rise, the weighted averages of HC drop. On the other hand, if HHO gas flow rates increase and are then added to the B40D60 blend, it results in a considerable reduction in HC values.

2.2 Weighted average of CO<sub>2</sub>

As shown in the figure [31], the most weighted average value of CO<sub>2</sub> at D100 is 4.7204%, whereas the least value is found with 2.5097% of B40D60 + HHO [15 LPM] as compared to other used mixtures, so the 40% biodiesel and diesel blend plus oxyhydrogen gas with a flow rate of 15 LPM is the best weighted average record to use. As various biodiesel and diesel blends rise, the weighted averages of CO<sub>2</sub> drop. On the other hand, if HHO gas flow

rates increase and are then added to the B40D60 blend, it results in a considerable reduction in CO<sub>2</sub> values.

### 2.3 Weighted average of CO

As shown in the figure [32], the most weighted average value of CO at D100 is 0.384%, whereas the least value is found with 0.152% of B40D60 + HHO [15 LPM] as compared to other used mixtures, so the 40% biodiesel and diesel blend plus oxyhydrogen gas with a flow rate of 15 LPM is the best weighted average record to use. As various biodiesel and diesel blends rise, the weighted averages of CO drop. On the other hand, if HHO gas flow rates increase and are then added to the B40D60 blend, it results in a considerable reduction in CO values.

### 2.4 Weighted average of O<sub>2</sub>

As shown in the figure [33], the most weighted average value of O<sub>2</sub> at D100 is 16.17%, whereas the least value is found with 12.07% of B40D60 + HHO [15 LPM] as compared to other used mixtures, so the 40% biodiesel and diesel blend plus oxyhydrogen gas with a flow rate of 15 LPM is the best weighted average record to use. As various biodiesel and diesel blends rise, the weighted averages of O<sub>2</sub> drop. On the other hand, if HHO gas flow rates increase and are then added to the B40D60 blend, it results in a considerable reduction in O<sub>2</sub> values.

### 2.5 Weighted average of NO<sub>x</sub>

As shown in the figure [34], the most weighted average value of NO<sub>x</sub> at D100 is 549.5 PPM, whereas the least value is found with 371.5 PPM of B40D60 + HHO [15 LPM] as compared to other used mixtures, so the 40% biodiesel and diesel blend plus oxyhydrogen gas with a flow rate of 15 LPM is the best weighted average record to use. As various biodiesel and diesel blends rise, the weighted averages of NO<sub>x</sub> drop. On the other hand, if HHO gas flow rates increase and are then added to the B40D60 blend, it results in a considerable reduction in NO<sub>x</sub> values.

### 2.6 Weighted average of soot

As shown in the figure [35], the most weighted average value of soot at D100 is 53.4885%, whereas the least value is found with 26.7266% of B40D60 + HHO [15 LPM] as compared to other used mixtures, so the 40% biodiesel and diesel blend plus oxyhydrogen gas with a flow rate of 15 LPM is the best weighted average record to use. As various biodiesel and diesel blends rise, the weighted averages of soot drop. On the other hand, if HHO gas flow rates increase and are then added to the B40D60 blend, it results in a considerable reduction in soot values.

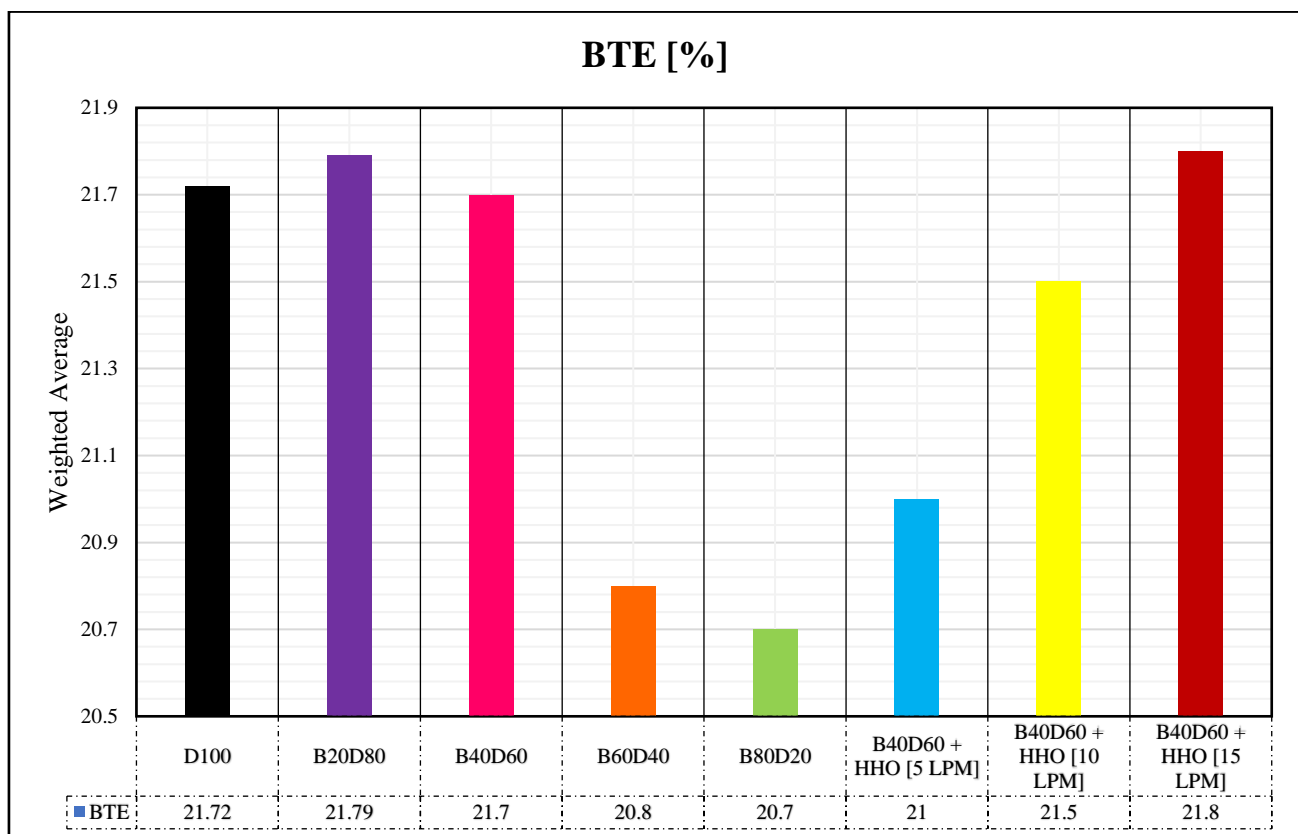


Figure 27: BTE weighted average values.

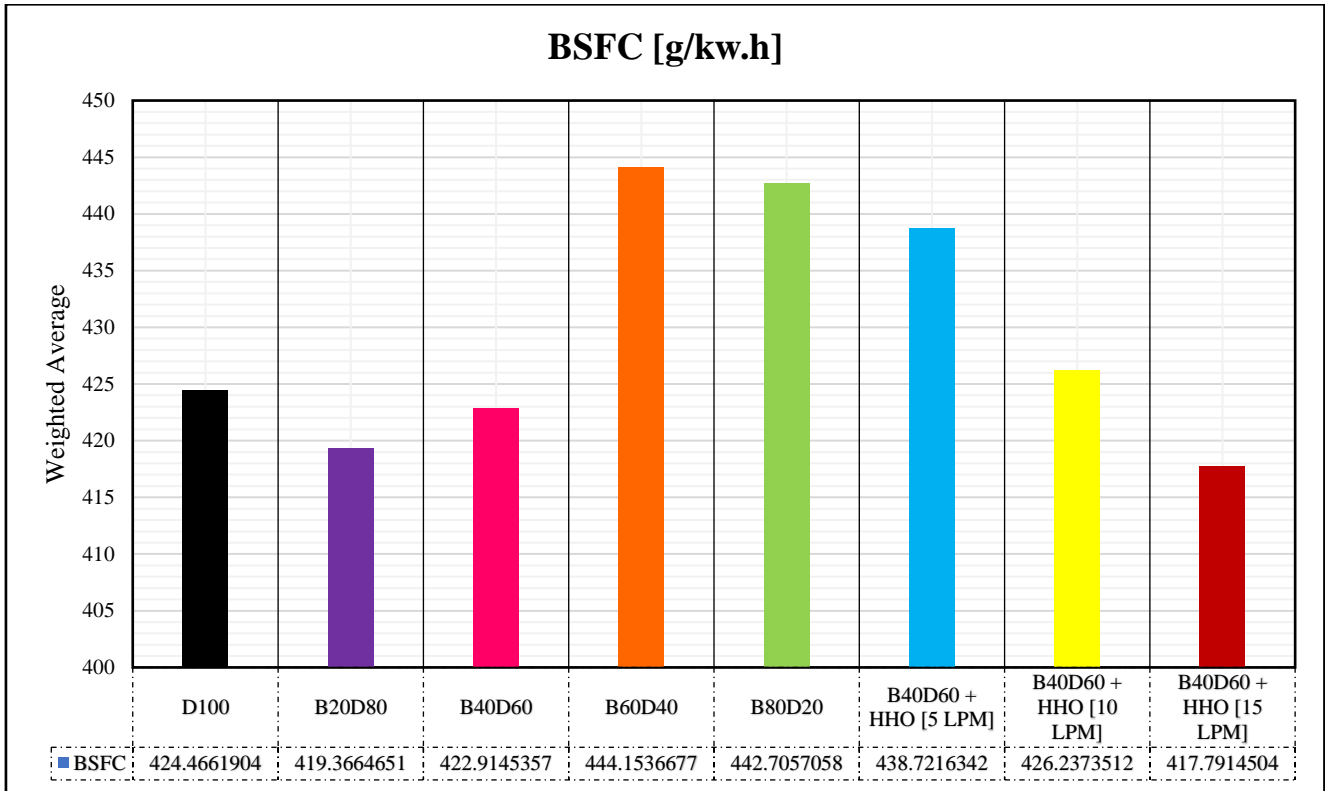


Figure 28: BSFC weighted average values.

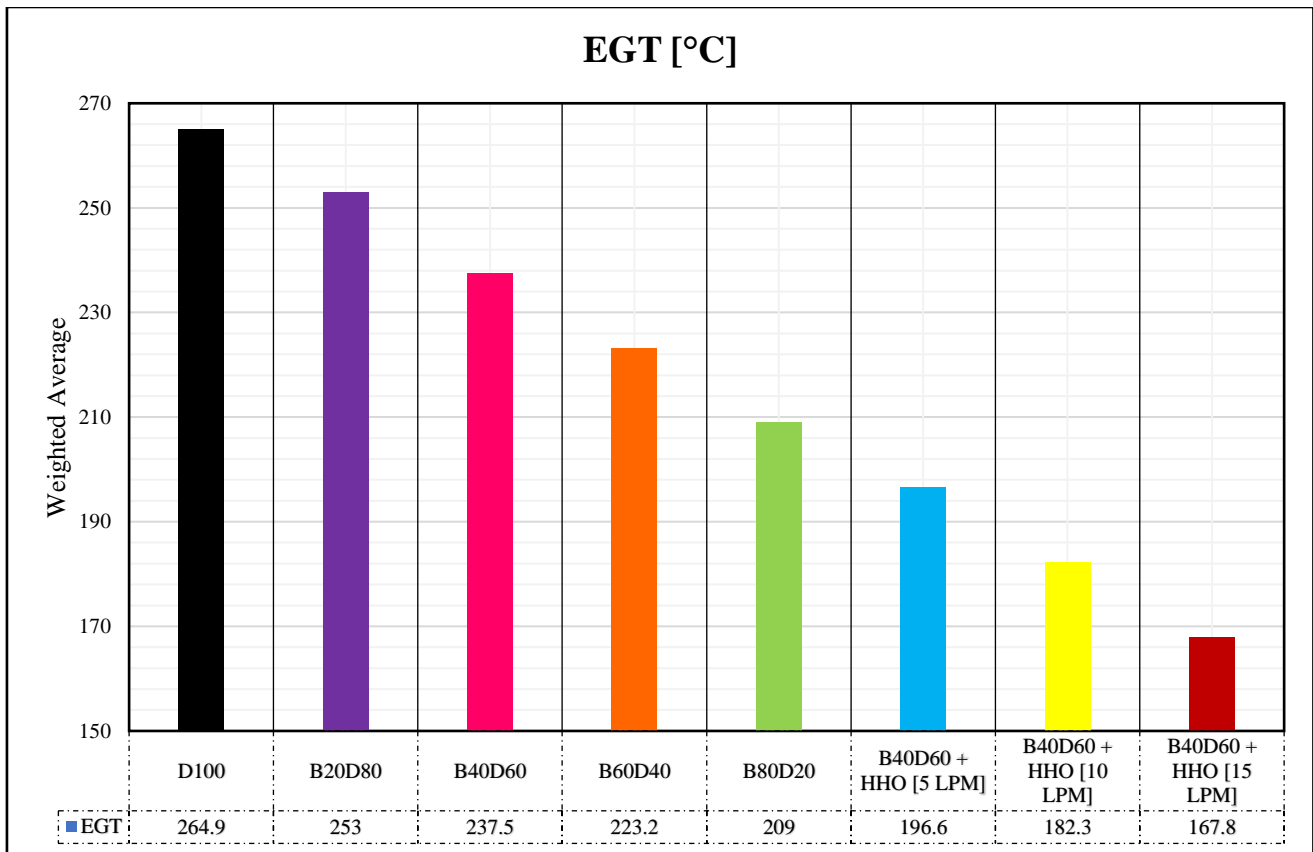


Figure 29: EGT weighted average values.

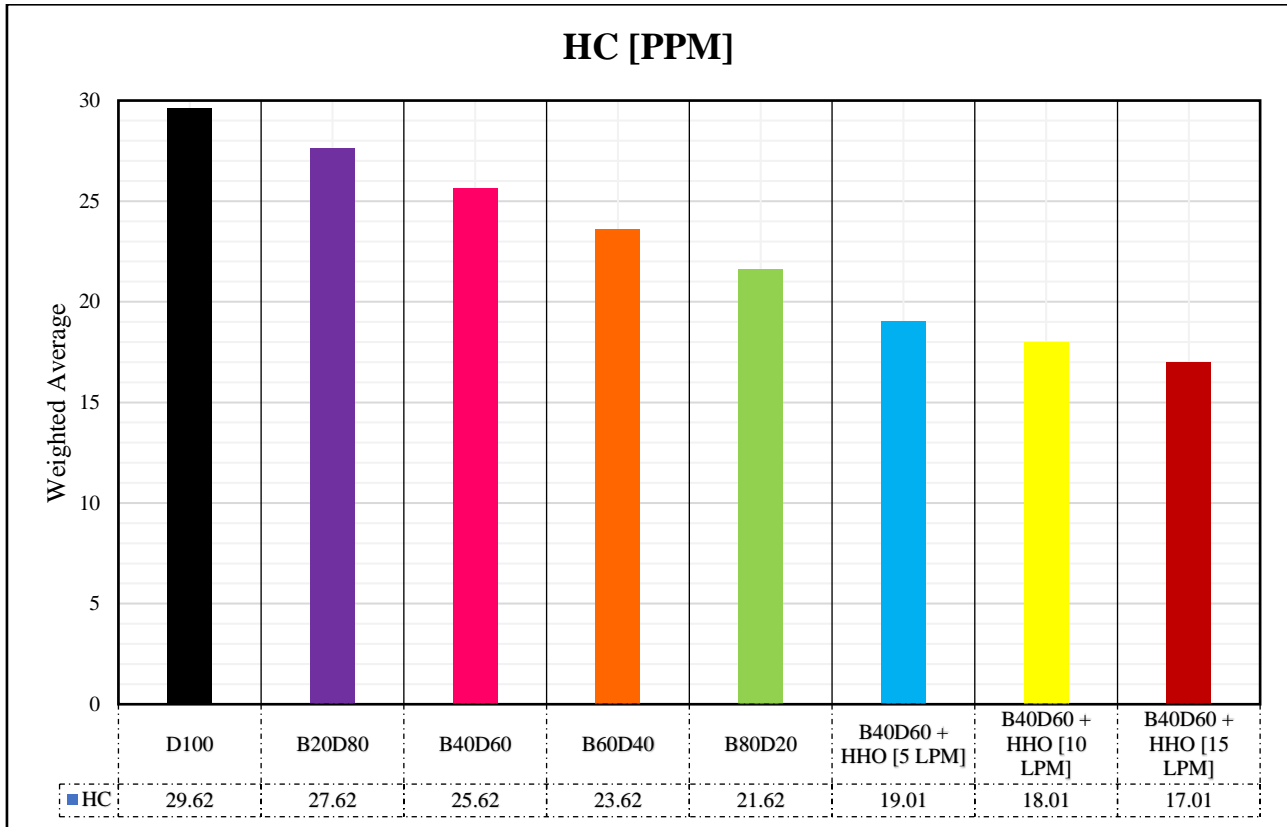


Figure 30: HC weighted average values.

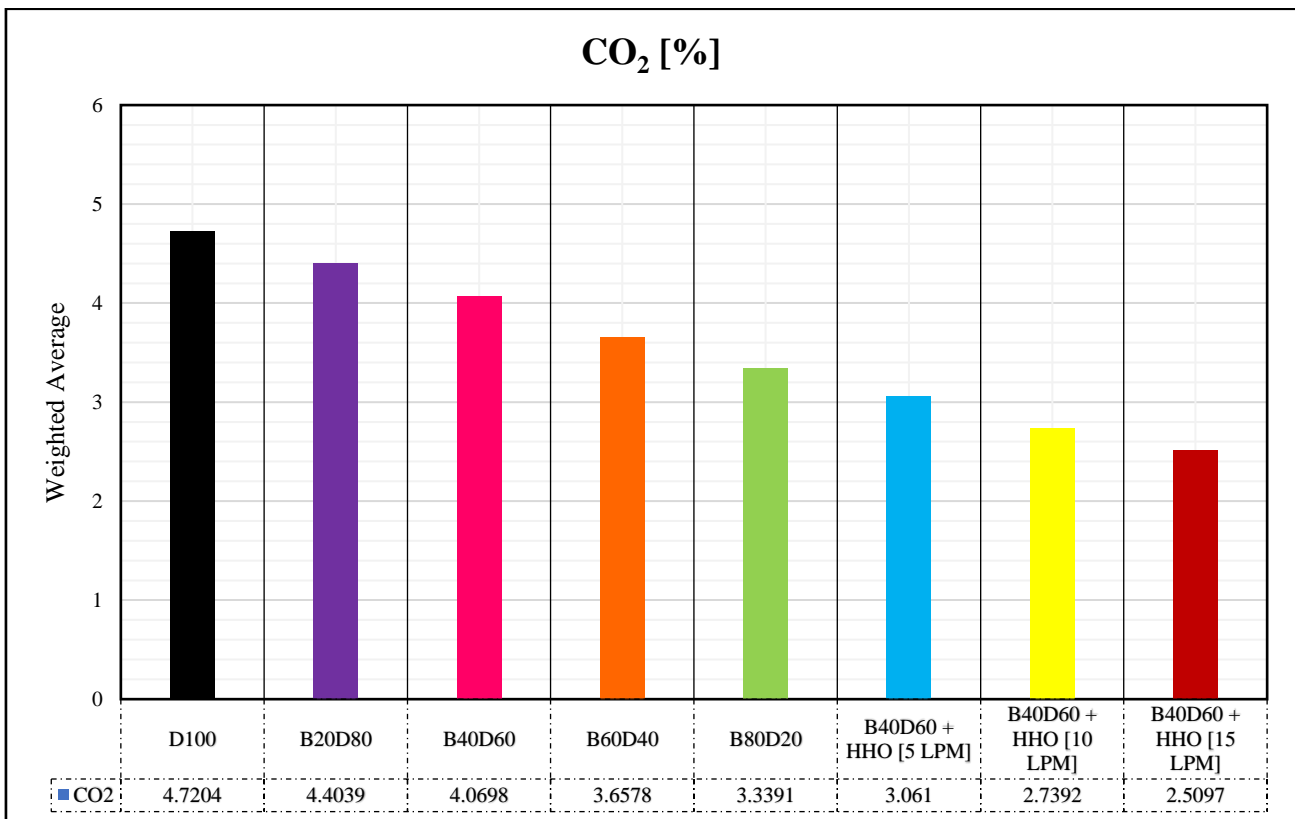


Figure 31: CO<sub>2</sub> weighted average values.

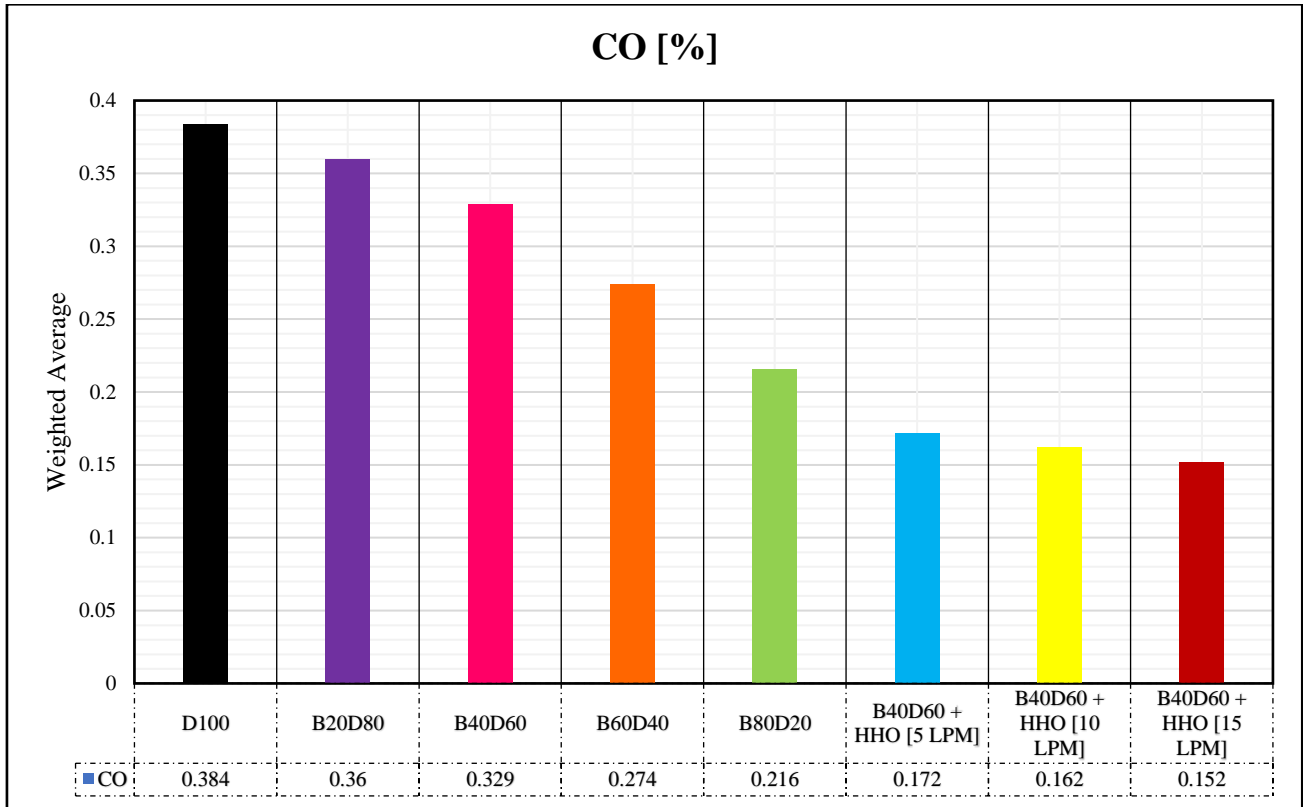


Figure 32: CO weighted average values.

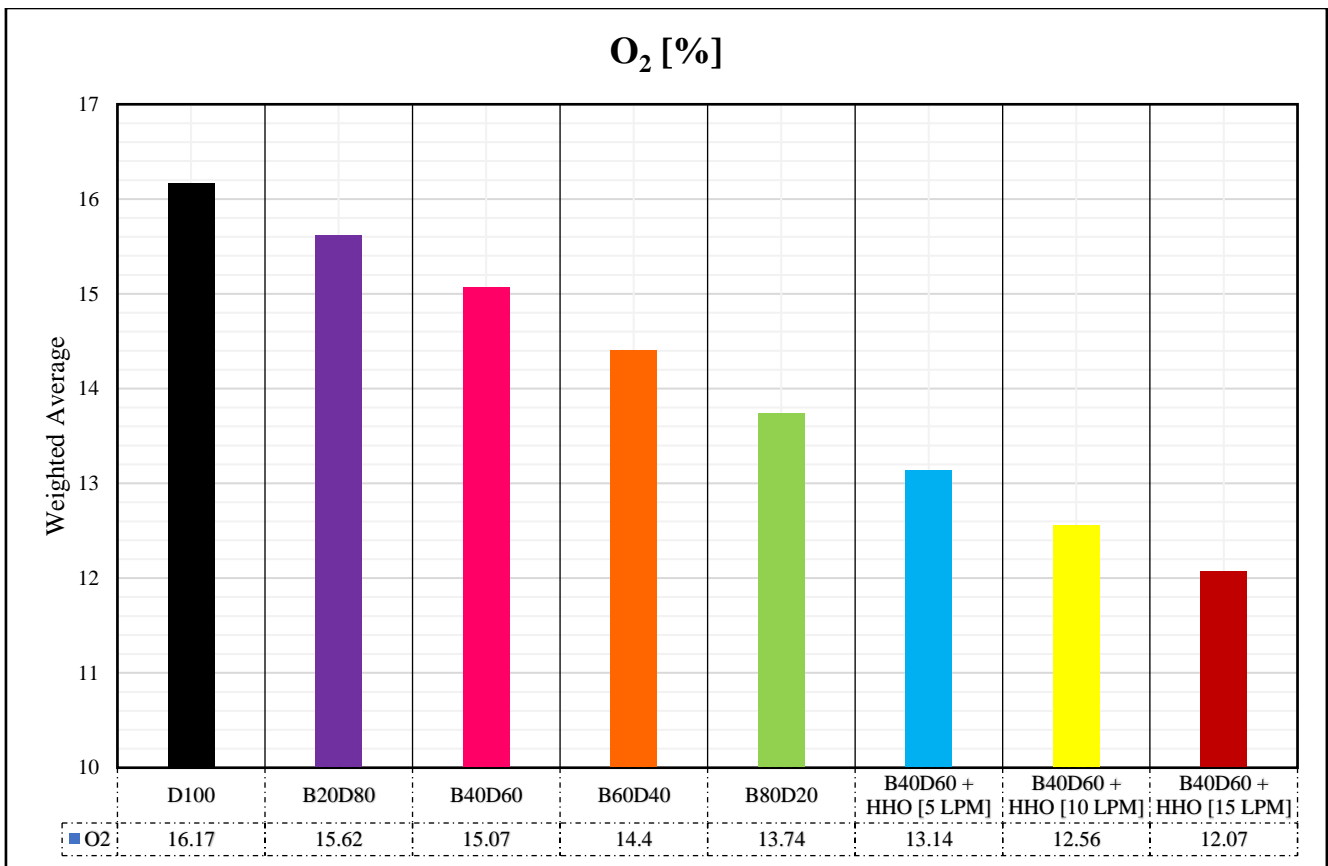


Figure 33: O<sub>2</sub> weighted average values.



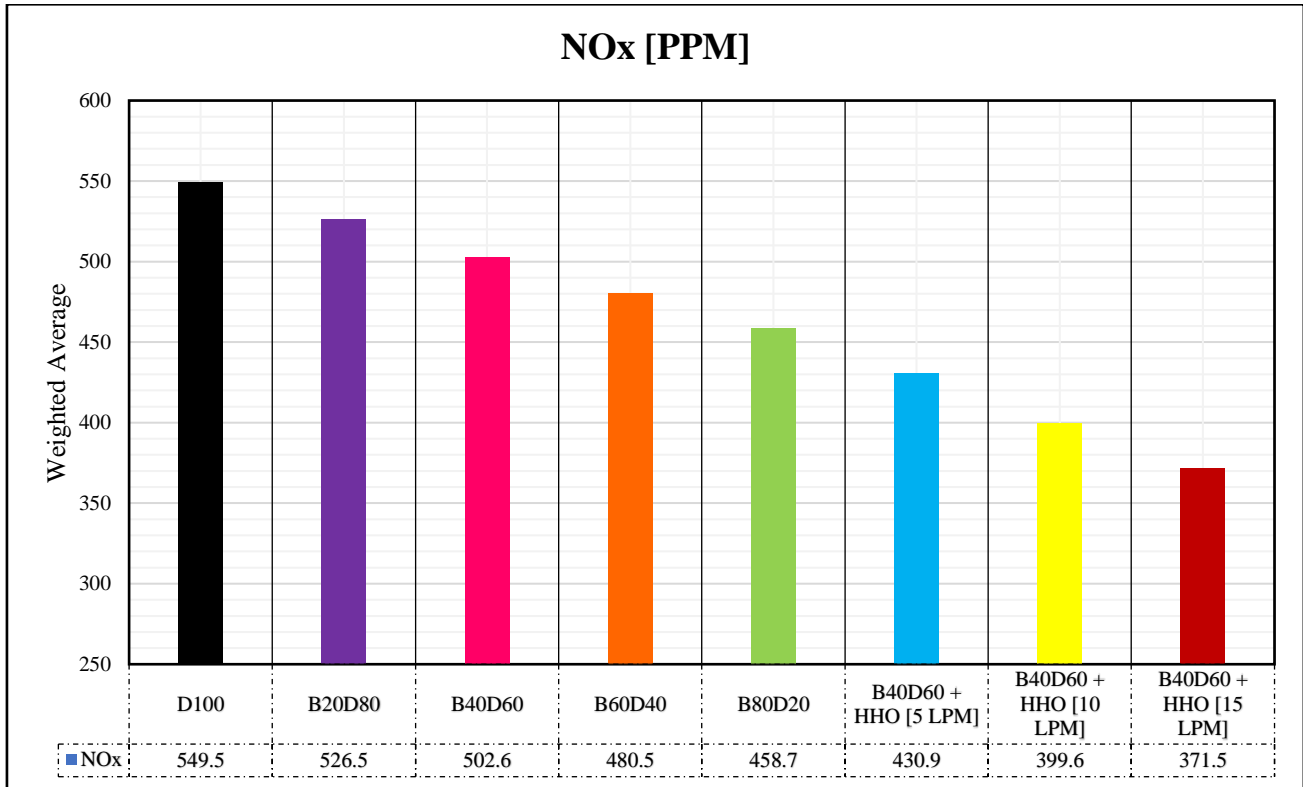


Figure 34: NO<sub>x</sub> weighted average values.

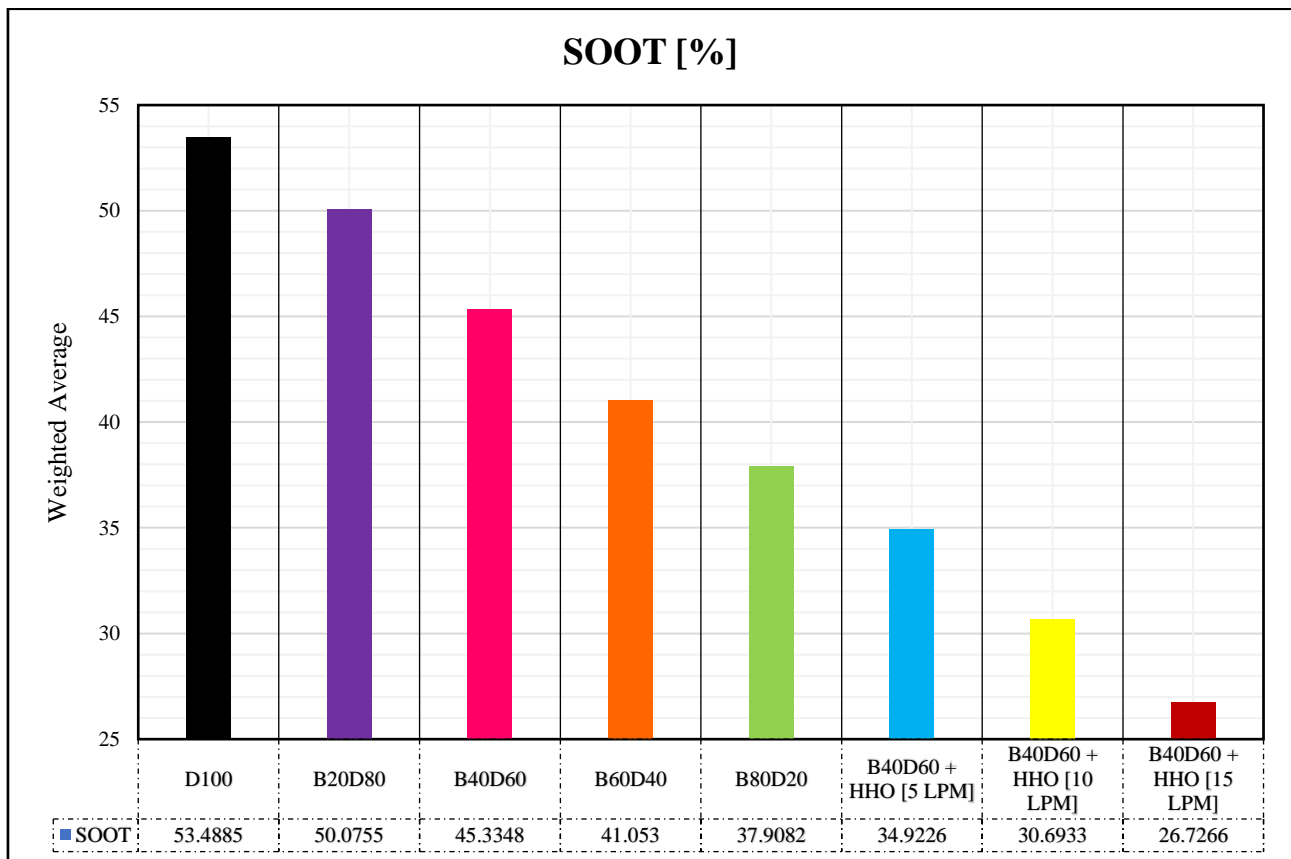


Figure 35: Soot weighted average values.

#### IV. CONCLUSION

This paper explains the impacts of the addition of different oxyhydrogen gas flow rates [5, 10, and 15%] with a 40% sunflower and soybean oil biodiesel and diesel blend on PCCI engine characteristics and compares the blends used by others. The conclusion from this investigation of this paper is that the experiment results observed that the parameters BTE, EGT, HC, CO<sub>2</sub>, CO, NO<sub>x</sub>, and soot rose, whereas there was a remarkable reduction in BSFC and O<sub>2</sub> for all test conditions.

- At 3.4866 KW of engine brake power, the 40% biodiesel/diesel blend has better performance characteristics than the addition of oxyhydrogen gas with 15 LPM of flow rate to the 40% biodiesel/diesel blend, which increases both BTE by 26.6% and EGT by 281%, but BSFC by 422.9145357 g/kw.h.
- The best outcome for exhaust emissions occurs when 15 LPM of flow rate of oxyhydrogen is added to 40% biodiesel and diesel blend by 23 PPM of HC, 3.42% of CO<sub>2</sub>, 0.25% of CO, 11.13% of O<sub>2</sub>, 539 PPM of NO<sub>x</sub>, and 55% of soot, at 3.4866 KW as compared to other mixtures used.
- The best weighted average outcome for BTE, BSFC, HC, CO<sub>2</sub>, CO, O<sub>2</sub>, NO<sub>x</sub>, and soot parameters is at B40D60 + HHO [15 LPM], whereas the worst value of them is at D100, so the 40% biodiesel and diesel blend plus oxyhydrogen gas with a flow rate of 15 LPM will be a more ideal weighted average to use. On the contrary, the best of the weighted average EGT values is at both D100 and B20D80, but the worst at B40D60 + HHO [15 LPM].
- The maximum weighted average BTE result at B40D60 + HHO [15 LPM] is 21.8%, while the minimum recorded at B80D20 is 20.7% when compared to other mixtures used.
- The maximum weighted average BSFC result at B60D40 is 444.1536677 g/kw.h, while the minimum recorded at of B40D60 + HHO [15 LPM] is 417.7914504 g/kw.h when compared to other mixtures used.
- The maximum weighted average EGT result at D100 is 264.9 °C, while the minimum recorded at of B40D60 + HHO [15 LPM] is 167.8 °C when compared to other mixtures used. However, the B20D80 weighted average is greater than the other test biodiesel/diesel blends, and it is also greater than the addition of 40% biodiesel/diesel blend to three flow rates [5, 10, and 15 LPM] of HHO gas, which results in the best temperature of the exhaust gas temperature parameter being 20% biodiesel/diesel blend.
- The maximum weighted average HC result at D100 is 29.62 PPM, while the minimum recorded at B40D60 + HHO [15 LPM] is 17.01 PPM when compared to other mixtures used.

- The maximum weighted average CO<sub>2</sub> result at D100 is 4.7204%, while the minimum recorded at B40D60 + HHO [15 LPM] is 2.5097 % when compared to other mixtures used.
- The maximum weighted average CO result at D100 is 0.384%, while the minimum recorded at B40D60 + HHO [15 LPM] is 0.152 % when compared to other mixtures used.
- The maximum weighted average O<sub>2</sub> result at D100 is 16.17%, while the minimum recorded at B40D60 + HHO [15 LPM] is 12.07 % when compared to other mixtures used.
- The maximum weighted average NO<sub>x</sub> result at D100 is 549.5 PPM while the minimum recorded at B40D60 + HHO [15 LPM] is 371.5 PPM when compared to other mixtures used.
- The maximum weighted average soot result at D100 is 53.4885%, while the minimum recorded at B40D60 + HHO [15 LPM] is 26.7266% when compared to other mixtures used.
- The previous authors offered many approaches for PCCI engines to improve the value of engine attributes such as performance and exhaust emissions. Future papers will employ technological approaches.

#### FUNDING:

Research was Funded by the administration at Tanta University under the number of: tu: 02-19-01.

#### REFERENCES

- [1] M. Elkelawy, S. E.-d. H. Etaiw, H. A.-E. Bastawissi, H. Marie, A. M. Radwan, M. M. Dawood, *et al.*, "WCO biodiesel production by heterogeneous catalyst and using cadmium (II)-based supramolecular coordination polymer additives to improve diesel/biodiesel fueled engine performance and emissions," *Journal of Thermal Analysis and Calorimetry*, vol. 147, pp. 6375-6391, 2022/06/01 2022.
- [2] A. M. Elzahaby, M. Elkelawy, H. A.-E. Bastawissi, S. M. El\_Malla, and A. M. M. Naceb, "Kinetic modeling and experimental study on the combustion, performance and emission characteristics of a PCCI engine fueled with ethanol-diesel blends," *Egyptian Journal of Petroleum*, vol. 27, pp. 927-937, 2018/12/01/ 2018.
- [3] S. C. Sekhar, K. Karuppusamy, R. Sathyamurthy, M. Elkelawy, H. A. E. D. Bastawissi, P. Paramasivan, *et al.*, "Emission analysis on compression ignition engine fueled with lower concentrations of Pithecellobium dulce biodiesel-diesel blends," *Heat Transfer—Asian Research*, vol. 48, pp. 254-269, 2019.
- [4] M. Elkelawy, S. E.-d. H. Etaiw, H. Alm-Eldin Bastawissi, M. I. Ayad, A. M. Radwan, and M. M. Dawood, "Diesel/biodiesel /silver thiocyanate nanoparticles/hydrogen peroxide blends as new fuel for enhancement of performance, combustion, and Emission characteristics of a diesel engine," *Energy*, vol. 216, p. 119284, 2021/02/01/ 2021.
- [5] M. Elkelawy, E. El Shennawy, H. Bastawissi, and I. El Shennawy, "The effect of using the WCO biodiesel as an alternative fuel in compression ignition diesel engine on

- performance and emissions characteristics," in *Journal of Physics: Conference Series*, 2022, p. 012023.
- [6] M. Elkelawy, S. E.-d. H. Etaiw, M. I. Ayad, H. Marie, M. Dawood, H. Panchal, *et al.*, "An enhancement in the diesel engine performance, combustion, and emission attributes fueled by diesel-biodiesel and 3D silver thiocyanate nanoparticles additive fuel blends," *Journal of the Taiwan Institute of Chemical Engineers*, vol. 124, pp. 369-380, 2021/07/01/ 2021.
- [7] M. Elkelawy, S. E.-d. H. Etaiw, H. A.-E. Bastawissi, H. Marie, A. Elbanna, H. Panchal, *et al.*, "Study of diesel-biodiesel blends combustion and emission characteristics in a CI engine by adding nanoparticles of Mn (II) supramolecular complex," *Atmospheric Pollution Research*, vol. 11, pp. 117-128, 2020/01/01/ 2020.
- [8] P. J. Megfa, A. J. Vizcaíno, J. A. Calles, and A. Carrero, "Hydrogen Production Technologies: From Fossil Fuels toward Renewable Sources. A Mini Review," *Energy & Fuels*, vol. 35, pp. 16403-16415, 2021/10/21 2021.
- [9] H. A. E. Bastawissi, M. Elkelawy, H. Panchal, and K. Kumar Sadasivuni, "Optimization of the multi-carburant dose as an energy source for the application of the HCCI engine," *Fuel*, vol. 253, pp. 15-24, 2019/10/01/ 2019.
- [10] M. Elkelawy, H. A.-E. Bastawissi, E. A. El Shenawy, M. M. Shams, H. Panchal, K. K. Sadasivuni, *et al.*, "Influence of lean premixed ratio of PCCI-DI engine fueled by diesel/biodiesel blends on combustion, performance, and emission attributes; a comparison study," *Energy Conversion and Management: X*, vol. 10, p. 100066, 2021/06/01/ 2021.
- [11] N. Patil, C. Chavan, A. More, and P. Baskar, "Generation of oxy-hydrogen gas and its effect on performance of spark ignition engine," in *IOP Conference Series: Materials Science and Engineering*, 2017, p. 062036.
- [12] M. Elkelawy, A. E. Kabeel, E. A. El Shenawy, H. Panchal, A. Elbanna, H. A.-E. Bastawissi, *et al.*, "Experimental investigation on the influences of acetone organic compound additives into the diesel/biodiesel mixture in CI engine," *Sustainable Energy Technologies and Assessments*, vol. 37, p. 100614, 2020/02/01/ 2020.
- [13] M. Elkelawy, E. A. El Shenawy, H. Alm-Eldin Bastawissi, M. M. Shams, and H. Panchal, "A comprehensive review on the effects of diesel/biofuel blends with nanofluid additives on compression ignition engine by response surface methodology," *Energy Conversion and Management: X*, vol. 14, p. 100177, 2022/05/01/ 2022.
- [14] E. A. El Shenawy, M. Elkelawy, H. A.-E. Bastawissi, M. M. Shams, H. Panchal, K. Sadasivuni, *et al.*, "Investigation and performance analysis of water-diesel emulsion for improvement of performance and emission characteristics of partially premixed charge compression ignition (PPCCI) diesel engines," *Sustainable Energy Technologies and Assessments*, vol. 36, p. 100546, 2019/12/01/ 2019.
- [15] E. A. El Shenawy, M. Elkelawy, H. A.-E. Bastawissi, H. Panchal, and M. M. Shams, "Comparative study of the combustion, performance, and emission characteristics of a direct injection diesel engine with a partially premixed lean charge compression ignition diesel engines," *Fuel*, vol. 249, pp. 277-285, 2019/08/01/ 2019.
- [16] M. Elkelawy, H. Alm-Eldin Bastawissi, E. A. El Shenawy, M. Taha, H. Panchal, and K. K. Sadasivuni, "Study of performance, combustion, and emissions parameters of DI-diesel engine fueled with algae biodiesel/diesel/n-pentane blends," *Energy Conversion and Management: X*, vol. 10, p. 100058, 2021/06/01/ 2021.
- [17] A. Singh, S. Sinha, A. K. Choudhary, H. Panchal, M. Elkelawy, and K. K. Sadasivuni, "Optimization of performance and emission characteristics of CI engine fueled with Jatropa biodiesel produced using a heterogeneous catalyst (CaO)," *Fuel*, vol. 280, p. 118611, 2020/11/15/ 2020.
- [18] S. Chandra Sekhar, K. Karuppasamy, N. Vedaraman, A. E. Kabeel, R. Sathyamurthy, M. Elkelawy, *et al.*, "Biodiesel production process optimization from Pithecellobium dulce seed oil: Performance, combustion, and emission analysis on compression ignition engine fuelled with diesel/biodiesel blends," *Energy Conversion and Management*, vol. 161, pp. 141-154, 2018/04/01/ 2018.
- [19] M. Elkelawy, H. A.-E. Bastawissi, K. K. Esmail, A. M. Radwan, H. Panchal, K. K. Sadasivuni, *et al.*, "Maximization of biodiesel production from sunflower and soybean oils and prediction of diesel engine performance and emission characteristics through response surface methodology," *Fuel*, vol. 266, p. 117072, 2020/04/15/ 2020.
- [20] M. Elkelawy, H. Alm-Eldin Bastawissi, K. K. Esmail, A. M. Radwan, H. Panchal, K. K. Sadasivuni, *et al.*, "Experimental studies on the biodiesel production parameters optimization of sunflower and soybean oil mixture and DI engine combustion, performance, and emission analysis fueled with diesel/biodiesel blends," *Fuel*, vol. 255, p. 115791, 2019/11/01/ 2019.
- [21] A. Dewangan, A. Mallick, A. K. Yadav, S. Islam, C. A. Saleel, S. Shaik, *et al.*, "Production of oxy-hydrogen gas and the impact of its usability on CI engine combustion, performance, and emission behaviors," *Energy*, vol. 278, p. 127937, 2023.
- [22] H. Thakkar, K. k. Sadasivuni, P. V. Ramana, H. Panchal, M. Suresh, M. Israr, *et al.*, "Comparative analysis of the use of flash evaporator and solar still with a solar desalination system," *International Journal of Ambient Energy*, vol. 43, pp. 1561-1568, 2022/12/31 2022.
- [23] B. Kanimozhi, M. Alsehli, A. Elfasakhany, D. Veeman, S. Balaji, T. P. Kumar, *et al.*, "Effects of oxyhydrogen on the CI engine fueled with the biodiesel blends: A performance, combustion and emission characteristics study," *International Journal of Hydrogen Energy*, vol. 47, pp. 37668-37676, 2022.
- [24] A. E. Kabeel, M. Elkelawy, H. A.-E. Mohamad, A. M. Elbanna, H. Panchal, M. Suresh, *et al.*, "The influences of loading ratios and conveying velocity on gas-solid two phase flow characteristics: a comprehensive experimental CFD-DEM study," *International Journal of Ambient Energy*, vol. 43, pp. 2714-2726, 2022/12/31 2022.
- [25] M. Elkelawy, E. A. El Shenawy, H. A. E. Bastawissi, and I. A. El Shennawy, "The effect of using the WCO biodiesel as an alternative fuel in compression ignition diesel engine on performance and emissions characteristics," *Journal of Physics: Conference Series*, vol. 2299, p. 012023, 2022/07/01 2022.
- [26] J. G. Vaghasia, J. K. Ratnadhariya, H. Panchal, K. K. Sadasivuni, D. Ponnamma, M. Elkelawy, *et al.*, "Experimental performance investigations on various orientations of evacuated double absorber tube for solar parabolic trough concentrator," *International Journal of Ambient Energy*, vol. 43, pp. 492-499, 2022/12/31 2022.
- [27] M. Elkelawy, H. A.-E. Bastawissi, E.-S. A. El-Shenawy, H. Panchal, K. Sadasivuni, D. Ponnamma, *et al.*, "Experimental investigations on spray flames and emissions analysis of diesel and diesel/biodiesel blends for combustion

- in oxy-fuel burner," *Asia-Pacific Journal of Chemical Engineering*, vol. 14, p. e2375, 2019.
- [28] D. Sekar, G. Venkadesan, and M. S. Panithasan, "Optimisation of dry cell electrolyser and hydroxy gas production to utilise in a diesel engine operated with blends of orange peel oil in dual-fuel mode," *International Journal of Hydrogen Energy*, vol. 47, pp. 4136-4154, 2022.
- [29] A. Mohammed Elbanna, C. Xiaobei, Y. Can, M. Elkelawy, H. Alm-Eldin Bastawissi, and H. Panchal, "Fuel reactivity controlled compression ignition engine and potential strategies to extend the engine operating range: A comprehensive review," *Energy Conversion and Management: X*, vol. 13, p. 100133, 2022/01/01/ 2022.
- [30] M. Elkelawy, "Experimental Investigation of Intake Diesel Aerosol Fuel Homogeneous Charge Compression Ignition (HCCI) Engine Combustion and Emissions," *Energy and Power Engineering*, vol. Vol.06No.14, p. 14, 2014.
- [31] M. Elkelawy, Z. Yu-Sheng, A. E.-D. Hagar, and J.-z. Yu, "Challenging and Future of Homogeneous Charge Compression Ignition Engines; an Advanced and Novel Concepts Review," *Journal of Power and Energy Systems*, vol. 2, pp. 1108-1119, 2008.
- [32] M. Elkelawy, E. A. El Shenawy, S. A. Mohamed, M. M. Elarabi, and H. A.-E. Bastawissi, "Impacts of using EGR and different DI-fuels on RCCI engine emissions, performance, and combustion characteristics," *Energy Conversion and Management: X*, vol. 15, p. 100236, 2022/08/01/ 2022.
- [33] M. M. El-Sheekh, M. Y. Bedaiwy, A. A. El-Nagar, M. ElKelawy, and H. Alm-Eldin Bastawissi, "Ethanol biofuel production and characteristics optimization from wheat straw hydrolysate: Performance and emission study of DI-diesel engine fueled with diesel/biodiesel/ethanol blends," *Renewable Energy*, vol. 191, pp. 591-607, 2022/05/01/ 2022.
- [34] M. Elkelawy, H. Alm Eldin Mohamad, and M. A. El-Gamal, "Experimental Investigation of the Biodiesel Direct Injection and Diesel Fuel as Premixed Charge on CI-Engine Emissions, Performance, and Combustion Characteristics," *Journal of Engineering Research*, vol. 7, pp. 177-187, 2023.
- [35] M. Elkelawy, E. A. El Shenawy, S. A. Mohamed, M. M. Elarabi, and H. Alm-Eldin Bastawissi, "Impacts of EGR on RCCI engines management: A comprehensive review," *Energy Conversion and Management: X*, vol. 14, p. 100216, 2022/05/01/ 2022.
- [36] E. A. El Shenawy, M. Elkelawy, H. A.-E. Bastawissi, M. Taha, H. Panchal, K. k. Sadasivuni, *et al.*, "Effect of cultivation parameters and heat management on the algae species growth conditions and biomass production in a continuous feedstock photobioreactor," *Renewable Energy*, vol. 148, pp. 807-815, 2020/04/01/ 2020.
- [37] J.-z. Yu, Z. Yu-Sheng, M. Elkelawy, and Q. Kui, "Spray and combustion characteristics of HCCI engine using DME/diesel blended fuel by port-injection," SAE Technical Paper 0148-7191, 2010.
- [38] H. A. El-Din, M. Elkelawy, and Z. Yu-Sheng, "HCCI engines combustion of CNG fuel with DME and H 2 additives," SAE Technical Paper 0148-7191, 2010.
- [39] M. Nibin, J. B. Raj, and V. E. Geo, "Experimental studies to improve the performance, emission and combustion characteristics of wheat germ oil fuelled CI engine using bioethanol injection in PCCI mode," *Fuel*, vol. 285, p. 119196, 2021/02/01/ 2021.
- [40] M. Elkelawy, Z. Yu-Sheng, H. A. El-Din, and Y. Jing-zhou, "A comprehensive modeling study of natural gas (HCCI) engine combustion enhancement by using hydrogen addition," SAE Technical Paper 0148-7191, 2008.
- [41] M. Elkelawy, H. Bastawissi, S. C. Sekar, K. Karuppasamy, N. Vedaraman, K. Sathiyamoorthy, *et al.*, "Numerical and experimental investigation of ethyl alcohol as oxygenator on the combustion, performance, and emission characteristics of diesel/cotton seed oil blends in homogenous charge compression ignition engine," SAE Technical Paper 0148-7191, 2018.
- [42] H. Wen, C. Wang, M. Elkelawy, and G. Jiang, "Influence of ambient pressure on gas ingestion in diesel nozzle after end of injection," *Trans. Chin. Soc. Agri. Mach*, vol. 48, pp. 364-369, 2017.
- [43] M. Elkelawy, H. Alm Eldin Mohamad, A. K. Abdel-Rahman, A. Abou Elyazied, and S. Mostafa El malla, "Biodiesel as an Alternative Fuel in Terms of Production, Emission, Combustion Characteristics for Industrial Burners: a Review," *Journal of Engineering Research*, vol. 6, pp. 45-52, 2022.
- [44] M. Elkelawy, H. Alm Eldin Mohamad, M. Samadony, A. M. Elbanna, and A. M. S. M. Safwat, "A Comparative Study on Developing the Hybrid-Electric Vehicle Systems and its Future Expectation over the Conventional Engines Cars," *Journal of Engineering Research*, vol. 6, pp. 21-34, 2022.
- [45] M. Elkelawy, Z. Yu-Sheng, H. El-Din, Y. Jing-Zhou, A. El Zahaby, and E. El Shenawy, "Experimental Study on Flash Boiling and Micro-Explosion of Emulsified Diesel Fuel Spray Droplets by Shadowgraph Technology," *Transactions of CSICE*, vol. 27, pp. 306-308, 2009.
- [46] S. F. Abd El Fattah, M. F. Ezzat, M. A. Mourad, M. Elkelawy, and I. M. Youssef, "Experimental Investigation of the Performance and Exhaust Emissions of a Spark-Ignition Engine Operating with Different Proportional Blends of Gasoline and Water Ammonia Solution," *Journal of Engineering Research*, vol. 5, pp. 38-45, 2022.
- [47] M. M. El-Sheekh, A. A. El-Nagar, M. ElKelawy, and H. A.-E. Bastawissi, "Maximization of bioethanol productivity from wheat straw, performance and emission analysis of diesel engine running with a triple fuel blend through response surface methodology," *Renewable Energy*, vol. 211, pp. 706-722, 2023/07/01/ 2023.
- [48] M. M. El-Sheekh, A. A. El-Nagar, M. ElKelawy, and H. A.-E. Bastawissi, "Bioethanol from wheat straw hydrolysate solubility and stability in waste cooking oil biodiesel/diesel and gasoline fuel at different blends ratio," *Biotechnology for Biofuels and Bioproducts*, vol. 16, p. 15, 2023/02/01 2023.
- [49] H. A. El-Din, Y.-S. Zhang, and M. Elkelawy, "A computational study of cavitation model validity using a new quantitative criterion," *Chinese Physics Letters*, vol. 29, p. 064703, 2012.
- [50] E. El Shenawy, M. Elkelawy, H. A.-E. Bastawissi, and M. Shams, "EXPERIMENTAL STUDY ON THE PERFORMANCE AND EMISSION CHARACTERISTICS OF PCCI ENGINE FUELED WITH BIODIESEL/DIESEL BLENDS," *ERJ. Engineering Research Journal*, vol. 41, pp. 119-132, 2018.
- [51] M. Elkelawy, H. A.-E. Bastawissi, A. M. Radwan, M. T. Ismail, and M. El-Sheekh, "Chapter 15 - Biojet fuels production from algae: conversion technologies, characteristics, performance, and process simulation," in *Handbook of Algal Biofuels*, M. El-Sheekh and A. E.-F. Abomohra, Eds., ed: Elsevier, 2022, pp. 331-361.
- [52] S. El-din H. Etaiw, M. Elkelawy, I. Elziny, M. Taha, I. Veza, and H. Alm-Eldin Bastawissi, "Effect of nanocomposite

- SCPI additive to waste cooking oil biodiesel as fuel enhancer on diesel engine performance and emission characteristics," *Sustainable Energy Technologies and Assessments*, vol. 52, p. 102291, 2022/08/01/ 2022.
- [53] A. M. Elbanna, X. Cheng, C. Yang, M. Elkelawy, and H. Alm-Eldin Bastawissi, "Investigative research of diesel/ethanol advanced combustion strategies: A comparison of Premixed Charge Compression Ignition (PCCI) and Direct Dual Fuel Stratification (DDFS)," *Fuel*, vol. 345, p. 128143, 2023/08/01/ 2023.
- [54] H. Alm El-Din, M. Elkelawy, and A. E. Kabeel, "Study of combustion behaviors for dimethyl ether asan alternative fuel using CFD with detailed chemical kinetics," *Alexandria Engineering Journal*, vol. 56, pp. 709-719, 2017/12/01/ 2017.
- [55] H. A.-E. Bastawissi and M. Elkelawy, "Investigation of the Flow Pattern inside a Diesel Engine Injection Nozzle to Determine the Relationship between Various Flow Parameters and the Occurrence of Cavitation," *Engineering*, vol. Vol.06No.13, p. 13, 2014.
- [56] H. A. E.-D. Bastawissi and M. Elkelawy, "Computational Evaluation of Nozzle Flow and Cavitation Characteristics in a Diesel Injector," *SAE International Journal of Engines*, vol. 5, pp. 1605-1616, 2012.
- [57] A. E. Kabeel, M. Elkelawy, H. A. E. Bastawissi, and A. M. Elbanna, "An experimental and theoretical study on particles-in-air behavior characterization at different particles loading and turbulence modulation," *Alexandria Engineering Journal*, vol. 58, pp. 451-465, 2019/06/01/ 2019.
- [58] A. M. Elbanna, C. Xiaobei, Y. Can, M. Elkelawy, and H. A.-E. Bastawissi, "A comparative study for the effect of different premixed charge ratios with conventional diesel engines on the performance, emissions, and vibrations of the engine block," *Environmental Science and Pollution Research*, vol. 30, pp. 106774-106789, 2023/10/01 2023.
- [59] E. Ramachandran, R. Krishnaiah, E. Perumal Venkatesan, S. R. Medapati, and P. Sekar, "Experimental Investigation on the PCCI Engine Fueled by Algal Biodiesel Blend with CuO Nanocatalyst Additive and Optimization of Fuel Combination for Improved Performance and Reduced Emissions at Various Load Conditions by RSM Technique," *ACS Omega*, vol. 8, pp. 8019-8033, 2023/02/28 2023.
- [60] M. Elkelawy, H. Alm ElDin Mohamad, M. Samadony, and A. S. Abdalhadi, "Impact of Utilizing a Diesel/Ammonia Hydroxide Dual Fuel on Diesel Engines Performance and Emissions Characteristics," *Journal of Engineering Research*, vol. 7, pp. 262-271, 2023.
- [61] H. Alm ElDin Mohamad, M. Elkelawy, and M. Ramon, "Computational fluid dynamics study on a solar chimney with different ground materials," *Journal of Engineering Research*, vol. 7, pp. 176-185, 2023.
- [62] M. Elkelawy, H. Alm ElDin Mohamad, M. Samadony, and A. S. Abdalhadi, "Utilization of Ammonia Hydroxide /Diesel Fuel Blends in Partially Premixed Charge Compression Ignition (PPCCI) Engine: A Technical Review," *Journal of Engineering Research*, vol. 7, pp. 319-331, 2023.
- [63] M. M. El-Sheekh, A. A. El-Nagar, M. Elkelawy, and H. A.-E. Bastawissi, "Solubility and stability enhancement of ethanol in diesel fuel by using tri-n-butyl phosphate as a new surfactant for CI engine," *Scientific Reports*, vol. 13, p. 17954, 2023/10/20 2023.
- [64] M. Elkelawy, H. A. Bastawissi, A. K. Abdel-Rahman, A. Abou-elyazied, and S. El-malla, "Experimental investigation of the effects of diesel-bioethanol blends on combustion and emission characteristics in industrial burner," *Journal of Physics: Conference Series*, vol. 2616, p. 012018, 2023/11/01 2023.
- [65] M. Elkelawy, H. A. Bastawissi, E. A. El Shenawy, and M. A. M. El-Gamal, "Effects of using a novel fuel vaporizer on partially premixed charge compression ignition (PPCCI) engine emissions, performance, and combustion characteristics," *Journal of Physics: Conference Series*, vol. 2616, p. 012017, 2023/11/01 2023.
- [66] M. Elkelawy, E. S. A. El Shenawy, H. A.-E. Bastawissi, and M. M. Shams, "Impact of Carbon Nanotubes and Graphene Oxide Nanomaterials on the Performance and Emissions of Diesel Engine Fueled with Diesel/Biodiesel Blend," *Processes*, vol. 11, p. 3204, 2023.
- [67] M. Elkelawy, H. A.-E. Bastawissi, A. K. Abdel-Rahman, A. Abou El-Yazied, and S. Mostafa El malla, "Effect of multifunctional fuel additive in diesel/waste oil biodiesel blends on industrial burner flame performance and emission characteristics," *International Journal of Ambient Energy*, vol. 44, pp. 1382-1395, 2023/12/31 2023.
- [68] H. Alm ElDin Mohamad, E. Abd elhamid, M. Elkelawy, and O. Hendawi, "Experimental Investigation on the Effect of using Oxy-Hydrogen Gas on Spark Ignition Engines Performances, and Emissions Characteristic," *Journal of Engineering Research*, vol. 7, pp. 32-41, 2023.
- [69] M. Elkelawy, E. Abd elhamid, H. Alm ElDin Mohamad, S. Abo-Samra, and I. Abd-Elhay Elshennawy, "Nanoparticles Additives for Diesel/Biodiesel Fuel Blends as a Performance and Emissions Enhancer in the Applications of Direct Injection Diesel Engines: A comparative Review," *Journal of Engineering Research*, vol. 7, pp. 112-121, 2023.
- [70] M. Elkelawy, H. Alm ElDin Mohamad, E. Abd elhamid, and M. A. M. El-Gamal, "Experimental Investigation of the Biodiesel Direct Injection and Diesel Fuel as Premixed Charge on CI-Engine Emissions, Performance, and Combustion Characteristics," *Journal of Engineering Research*, vol. 7, pp. 177-187, 2023.
- [71] M. Elkelawy, A. Kamel, A. Abou-elyazied, and S. M. El-malla, "Experimental investigation of the effects of using biofuel blends with conventional diesel on the performance, combustion, and emission characteristics of an industrial burner," *Egyptian Sugar Journal*, vol. 19, pp. 44-59, 2022.
- [72] R. J. Moffat, "Describing the uncertainties in experimental results," *Experimental Thermal and Fluid Science*, vol. 1, pp. 3-17, 1988/01/01/ 1988.
- [73] S. H. Pourhoseini, M. Namvar-Mahboub, E. Hosseini, and A. Alimoradi, "A comparative exploration of thermal, radiative and pollutant emission characteristics of oil burner flame using palm oil biodiesel-diesel blend fuel and diesel fuel," *Energy*, vol. 217, p. 119338, 2021/02/15/ 2021.
- [74] M. Vijayaragavan, B. Subramanian, S. Sudhakar, and L. Natrayan, "Effect of induction on exhaust gas recirculation and hydrogen gas in compression ignition engine with simarouba oil in dual fuel mode," *International Journal of Hydrogen Energy*, vol. 47, pp. 37635-37647, 2022/10/30/ 2022.
- [75] M. Elkelawy, H. A.-E. Bastawissi, E. El Shenawy, M. Taha, H. Panchal, and K. K. Sadasivuni, "Study of performance, combustion, and emissions parameters of DI-diesel engine fueled with algae biodiesel/diesel/n-pentane blends," *Energy Conversion and Management: X*, vol. 10, p. 100058, 2021.